Surveying coconut trees using high-resolution satellite imagery in remote atolls of the Pacific Ocean

Juepeng Zheng [a,b], Shuai Yuan [b,d], Wenzhao Wu [c], Weijia Li [e], Le Yu [a,*], Haohuan Fu [a,b,c,**], David Coomes [f]

[a] Ministry of Education Key Laboratory for Earth System Modeling, Department of Earth System Science, Tsinghua University, Beijing, China
[b] Tsinghua University (Department of Earth System Science)-Xi'an Institute of Surveying and Mapping Joint Research Center for Next-Generation Smart Mapping, Beijing, China
[c] National Supercomputing Center in Wuxi, Wuxi, China
[d] Department of Electrical Engineering, City University of Hong Kong, Hong Kong, China
[e] School of Geospatial Engineering and Science, Sun Yat-Sen University, Zhuhai, China
[f] Conservation Research Institute and Department of Plant Sciences, Cambridge University, Downing Street, Cambridge CB2 3EA, UK

ARTICLE INFO

ABSTRACT

Coconut (*Cocos nucifera* L.) is one of the world's most economically important tree species, and coconut palm plantations dominate many islands and tropical coastlines. However, the expansion of plantations to supply international markets threatens biodiversity. Therefore, monitoring the plantations is important not only for the food industry but also for evaluating and mitigating environmental impacts of the industry. However, the detection of coconut trees from space is challenging because the palms' crowns hold only limited pixels of high-resolution optical imagery.

Here, we present an accurate and real-time COCOnut tree DETection method (COCODET) which uses satellite imagery to detect individual palms, comprising three components. First, an Adaptive Feature Enhancement (AFE) module is designed to improve both the capacity of representation at the highest level of the feature map and feature representation ability and help distinguish between coconut trees and other vegetation. Secondly, we modify a region proposal network to produce a Tree-shape Region Proposal Network (T-RPN) for producing coconut tree candidates. Finally, we create a Cross Scale Fusion (CSF) module for integrating multi-scale information to improve small tree detection; this fuses features of coconut crowns from different levels, connecting shallow and deep-level semantic features.

We applied COCODET to detect coconut trees in four remote atolls from the Acteon Group in French Polynesia. The natural habitats on the islands were previously cleared for coconut plantations, many of which have since been abandoned. COCODET achieved an average F1 score of 86.5% using its real-time inference process, considerably outperforming other cutting-edge object detection algorithms (4.3 ~ 12.0% more accurate). We detected 688 ha of coconuts and 182 ha of natural habitat on the islands, and within the coconut groves we detected 120,237 individuals. Our analyses indicate that deep learning approaches can be successfully applied to coconut palm detection, aiding efforts to understand human impacts on natural ecosystems and biodiversity.

1. Introduction

Coconut palm (*Cocos nucifera L.*) is among the world's most economically important tree species (Kappally et al., 2015). The palms are prominent on tropical islands (de Souza and Falcão, 2022) and other coastal regions. Coconut is one of the most versatile products in many tropical developing countries and has diverse uses as a vegetable oil, and as a component of food, fuel, medicine, carpets, building materials, and peat substitute. It is a significant source of revenue in many tropical coastal regions (Abankwah et al., 2010; Danso, 2017). However, the

expansion of coconut plantations to meet global demand is having serious consequences for biodiversity (Lathika and Ajith Kumar, 2005). According to Meijaard et al. (2020), to some extent, coconut plantations are more destructive than olive and oil palm plantations, with coconuts affecting 20 threatened species per million liters of oil produced, yet olive and palm oil only affecting 4.1 and 3.8 species per million liters, respectively.

While new plantations threaten wildlife, the management of old abandoned coconut groves is key for biodiversity protection on many islands (Pierce and Blanvillain, 2004). For example, the Ackeon Group of atolls in French Polynesia in the Pacific Ocean (Fig. 5) is home to several threatened and near-threatened bird species (Pierce and Blanvillain, 2004; Griffiths et al., 2008, 2011; Pott et al., 2014). Abandoned coconut plantations dominate the atolls, alongside remnants of relatively unmodified vegetation, such as the groves of pandanus (*Pandanus tectorius*) and mikimiki (*Pemphis acidula*). The abandoned plantations provide a vital habitat for many endangered bird species including the Polynesian ground-dove (*Gallicolumba erythroptera*) and Tuamotu sandpiper (*Prosobonia cancellata*) but also provide safe havens for Pacific rats (particularly black rat (*Rattus rattus*)) and cats (*Felis catus*) that eat the eggs of these birds (Griffiths et al., 2008). To this end, surveying coconut trees in these remote atolls of the Pacific Ocean is crucial to understand the habitats and environments of threatened bird species. (See Fig. 1.)

Remote surveying of individual trees to provide accurate information on locations and densities has many applications in forestry, food production and ecological assessments, and is already used to map coconuts (Rahnemoonfar and Sheppard, 2017). Rapid advances in high-resolution remote sensing from drones, aircraft and space alongside the development of new computational approaches have made it possible to automatically detect tree crowns from optical imagery (Hansen et al., 2013; Crowther et al., 2015; Brandt et al., 2018; Payne, 2021), and these approaches are now routinely used to estimate forest biomass, monitor environmental change and predict yields (Chong et al., 2017). Tree crown detection using high-resolution images has mostly been based on traditional image processing (Skurikhin et al., 2013; Xu et al., 2021b) or classical machine learning-based approaches (Selvaraj et al., 2020; Gleason and Im, 2012). More recently deep learning based methods have been used, including image classification-based method (Li et al., 2017; Zheng et al., 2020), semantic segmentation-based method (Osco et al., 2020; Zhang et al., 2020) and object detection-based method (Zheng et al., 2021a; Lumnitz et al., 2021). Deep learning has a greater capacity to extract feature and represent texture than previous image processing methods, often improving the accuracy and robustness.

Several algorithms have been developed specifically to recognize individual coconut trees (see Table 1). Most of existing algorithms are based on classical machine learning (Teina et al., 2008; Puttemans et al., 2018; Upendra et al., 2019; de Souza and Falcão, 2022), and image classification-based method (Vargas-Munoz et al., 2019) (see Table 1). For instance, Vermote et al. (2020) estimate the number of coconut trees in Tonga using the WorldView-3 images. Vargas-Munoz et al. (2019) argue that CNN classification is a feasible alternative for detecting palm trees as objects with high average accuracy in UAV imagery. However, these methods attain high accuracy, but use time-consuming sliding window technique that makes them inefficient when applied over large scales. As shown in the top line of Fig. 2, the sliding window technique requires a relatively large number of detected candidates of various sizes, splitting the entire image into many image patches with a specific window size and then classifying them as the background (other land cover types) or the tree crown through different CNN architectures. Furthermore, these methods are ineffective in detecting coconut palms of different crown sizes because the size of the image patch is predefined (Zheng et al., 2021a). Current studies have mapped no >30,000 trees, because of these limitations (see the number of detected trees in Table 1).

On the other hand, object detection-based approach is an end-to-end detection framework that aims to provide all detected objects for the whole image simultaneously (see the bottom line of Fig. 2), without timeconsuming sliding window technique and post-processing. Faster R-CNN is one of the most popular object detection-based approaches and have been applied in many tree crown detection applications (Zheng et al., 2021b). In general, the object detection-based approach is faster and more robust than for other types of tree crown detection methods, efficiently alleviating the performance drop caused by complex topography, confusion with other vegetation, etc. Up to now, only our previous work (Zheng et al., 2021b) adopts end-to-end detection framework with a high efficiency to achieve real-time coconut detection.

Deep learning has been successfully applied to detect objects such as ships (Liu et al., 2021; Zhang et al., 2021b), buildings (Li et al., 2019; Zhang et al., 2021a) and trees (Li et al., 2017; Hao et al., 2021), etc.). However, existing deep learning-based tree crown detection methods do not consider the characteristics of tree crowns in remote sensing images, and instead directly adopt common object detection frameworks. Detecting trees from high-resolution satellite imagery is challenging, because each tree is coarsely pixelated in the imagery, and densely packed canopies make it difficult to distinguish individuals. This makes tree detection distinct from other object detection tasks, such as detecting cats or dogs from photographs in the *COCO* dataset, where each object comprises thousands of pixels. Fig. 3 displays comparison of the complexity and difficulty in object size and density between a common object detection problem in the *COCO* dataset and a tree detection problem in remote sensing images (such as coconut trees and oil palm trees). Current deep learning approaches to tree-crown delineation adopt convolutional networks directly, without considering the coarse pixelation problem (see Table 1). As network architectures become deeper, the features of small trees may rarely appear in the deepest layers, leading to negative learning of tree crowns. Our previous work (Zheng et al., 2021b) adopted Faster R-CNN (Ren et al., 2016) and FPN (Lin et al., 2017) to complete coconut tree detection in Tenarunga, and achieved an F1 score of 77.1%, which is relatively poor (see Table 1). In this study, we further improve the algorithm to better detect small and dense tree crowns from remote sensing images (see Fig. 3) and expand our study area to include the whole Acteon Group in the Pacific Ocean. Therefore, our COCODET is much more effective and computationally efficient than existing coconut tree detection applications, making it possible to apply the algorithm over large spatial scales in real time. This paper makes the following contributions:

(1) We manually locate 120,237 coconut trees in French Polynesia from remote sensing images and those data with the codes are published on https://github.com/rs-dl/coconut_in_Acteon_Group. This is the largest available dataset of this sort for coconut trees.

(2) We present a high-accuracy, highly-efficient, real-time COCOnut

Number of species threatened by each oil crop per million tons of oil produced.
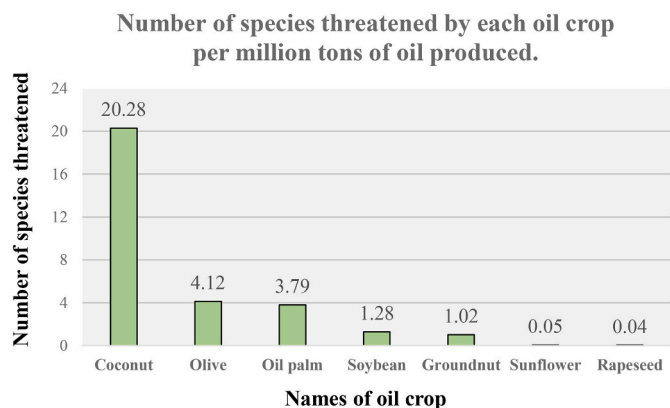

Fig. 1. The number of species threatened by each oil crop per million tons of oil produced (Meijaard et al., 2020).

Table 1
Summary of existing coconut tree detection studies.

Publications	Study site	No. trees	Imagery	Method	F1 score	End-to-end
Teina et al. (2008)	Tuamotu Archipelago	4133	IKONOS	SVM	69.1%[‖]	×
Puttemans et al. (2018)	-*	3798	Aerial images	Boosted Cascades	85.6%	×
Upendra et al. (2019)	Sri Lanka	–	UAV images	Template matching	90.0%[‖]	×
Vargas-Munoz et al. (2019)	Kingdom of Tonga	3144	8 cm UAV images	AlexNet	84.1%	×
Mohan et al. (2019)	Rio de Janeiro, Brazil	341	Lidar point clouds	adaptive TWS[†] approach	90.0%	×
Vermote et al. (2020)	Kingdom of Tonga	8926	WorldView-3	Shadow detection	93.0%[‖]	×
Zheng et al. (2021b)	Tenarunga	28,838	Google Earth	Faster R-CNN + FPN	77.1%	√
de Souza and Falcão (2022)	Kingdom of Tonga	10,268	8 cm UAV images	FLIM+MLP[#]	85.4%	×
This study	French Polynesia	120,573	Google Earth	COCODET	86.5%	√

[*] Unreported and unavailable values are labeled as '-'. [†]TWS denotes treetop window size.
[#] FLIM denotes feature learning from image markers; MLP denotes multilayer perceptron.
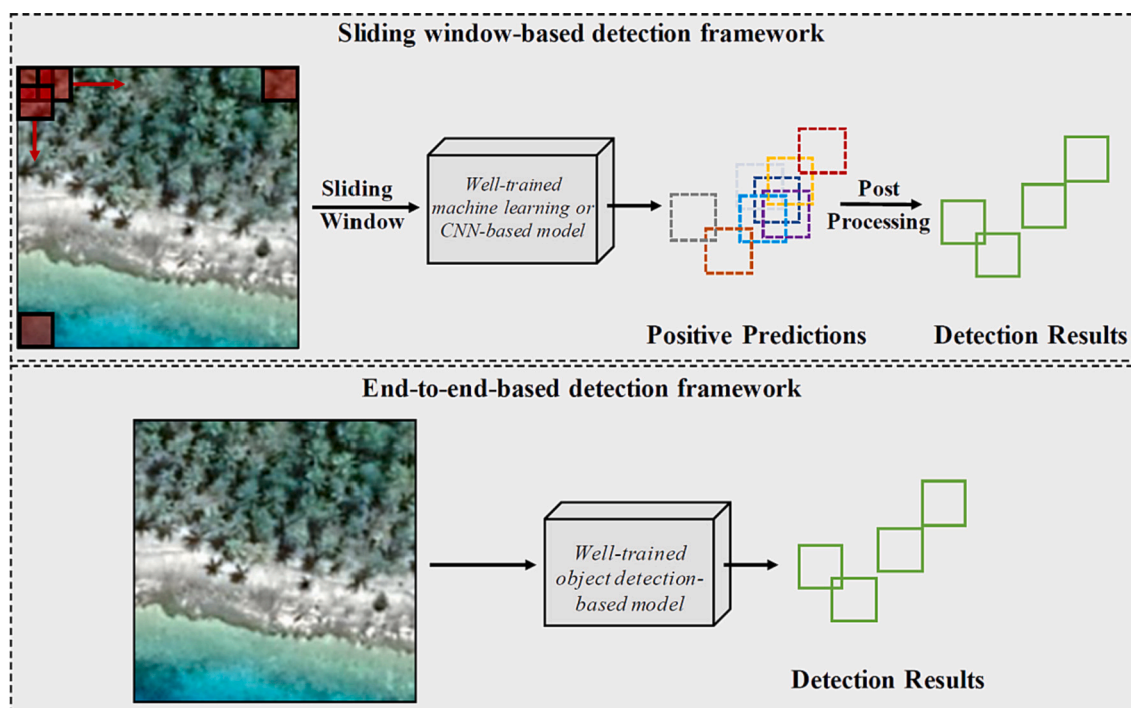[‖] denotes the publication reports the detection results with accuracy.

Fig. 2. Comparisons between sliding window-based detection framework (top line) and end-to-end-based detection framework (bottom line).
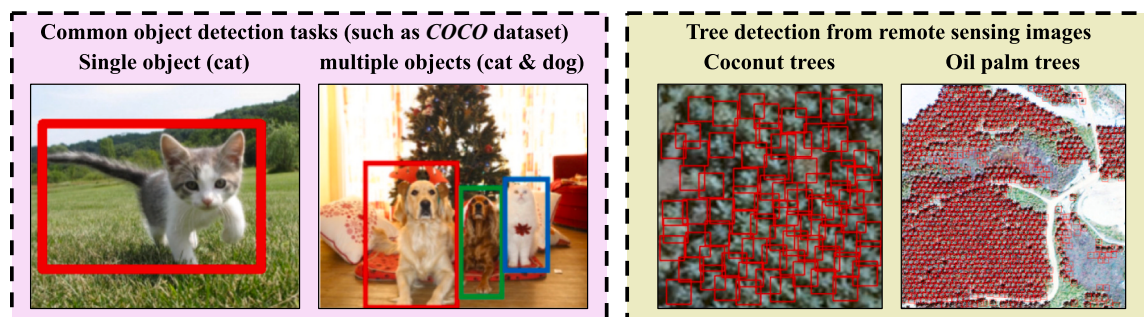

Fig. 3. Comparison of complexity and difficulty in object size and density between a common object detection problem in COCO dataset and a tree detection problem in remote sensing images (such as coconut trees and oil palm trees).

tree DETection method (COCODET). Our method includes three modules to solve the small-object problem where coconut stands are usually densely packed and individual trees: an Adaptive Feature Enhancement (AFE) module, a Tree-shape Region Proposal Network (T-RPN) and a Cross Scale Fusion module (CSF). These three novelties in COCODET are proposed to address limitations in existing methods for detecting small

and dense tree crowns from remote sensing images, which are really important in remote sensing object detection domain.

(3) We conduct a thorough survey of coconut trees for four remote atolls (Tenararo, Vahanga, Tenarunga and Matureivavao) in the Acteon Group from high-resolution satellite images. Our approach achieves an average F1 score of 86.5%, outperforming other cutting-edge object

detection algorithms (by 4.3 ∼ 12.0%).

(4) We provide more specific information on how coconut plantation can effect wildlife biodiversity, including their positive and negative impacts. We find that the Tenararo has much more amount of threatened bird species than the other three atolls, with the highest density and canopy area of the coconut plantations, which prove that the importance of coconut plantations for these endangered bird species.

In Sec.2 we briefly summarise previous work on Individual Tree Crown Detection (ITCD) domain, then present our proposed COCODET in Sec. 3. We introduce our study area, and demonstrate COCODET's performance in Sec. 4. After that, we discuss how coconut tree detection helps understand the ecological functions of coconut trees in the Acteon Group (Sec. 5). Finally, we conclude this paper in Sec. 6.

2. Overview of individual tree crown detection methods

Classical approaches to individual tree crown detection (see (Skurikhin et al., 2013; Hung et al., 2012)) use pattern recognition algorithms to extract handcrafted tree crown-like features, such as local maximum filtering (Xu et al., 2021b; Gebreslasie et al., 2011; Zheng et al., 2022b), image binarization (Koc-San et al., 2018; Pitkänen, 2001), image segmentation (Gougeon and Leckie, 2006; Santoso et al., 2016; Miraki et al., 2021), and template matching (Hung et al., 2012; Leckie et al., 2016; Norzaki and Tahar, 2019). Some researches prove that combining two or more methods may perform better ITCD results (Heenkenda et al., 2015) to achieve detecting and delineating tree crowns. For instance, Pitkänen (2001) combines locally adaptive binarization and local maximum filtering methods to achieve individual tree detection in digital aerial images, with 70 ∼ 95% of the trees were detected in sparse regions. Panagiotidis et al. (2017) combine local maximum filtering and inverse watershed segmentation to estimate crown diameters, achieving an acceptable accuracy for detecting tree crown diameter. Software tools are available for some classical approaches (Gebreslasie et al., 2011; Santoso et al., 2016) but their utility is limited by the need to tune many parameters and their lack of generality (Pitkänen, 2001). Many algorithms achieve high accuracy in sparse and simple regions, while have severe accuracy deterioration in dense and complex regions (Pitkänen, 2001).

Older machine learning methods have two components: feature extraction and classifier training. Extracted features can be generated through non-handcrafted methods, such as spectral information, vegetation indices such as Normalized Difference Vegetation Index, NDVI (Ouma and Tateishi, 2008) and texture characteristics (such as Gray-Level Co-occurrence Matrix, GLCM) (Pu and Landry, 2012), or can be handcrafted using methods including Histogram of Oriented Gradient (HOG) (Wang et al., 2019b) and Scale-Invariant Feature Transform (SIFT) (Malek et al., 2014). Popular adopted classifier contains decision tree (Ouma and Tateishi, 2008; Tochon et al., 2015), random forest (Selvaraj et al., 2020; Wallace et al., 2021) and Multi-Layer Perceptron (MLP) (Nevalainen et al., 2017), etc. Nevalainen et al. (2017) compare ITCD performance of 5 different classifiers including k-NN, Bayes classifier, decision tree, MLP and random forest. They build a high-resolution dataset based on hyperspectral and point cloud data, and extract about 350 features. Experimental results indicate that MLP achieves the best accuracy, followed by k-NN, random forest, decision tree and Bayes classifier. The generality of these older machine learning methods is stronger (Dalponte et al., 2014) but selecting suitable features for these methods is time consuming (Nevalainen et al., 2017) and performance is dependent on the quality of manually interpreted samples.

Many researchers have developed algorithms based on deep learning framework (LeCun et al., 2015), which can be used in large-scale applications with complex contexts to obtain good results. Deep learning of individual tree crowns has developed rapidly (Zheng et al., 2022a). Methods fall into three categories: (a) image classification (Guirado et al., 2017) using LeNet (Li et al., 2017; Wu et al., 2020b), AlexNet (Zheng et al., 2020; Nguyen et al., 2021), VGG (Safonova et al., 2019; de Souza and Falcão, 2022), and ResNet (Onishi and Ise, 2021); (b) Semantic Segmentation (Gurumurthy et al., 2019; Zhang et al., 2020) using DeepLabV3+ (Gibril et al., 2021), U-Net (Brandt et al., 2020) and Fully Connected Networks (Gurumurthy et al., 2019; Osco et al., 2021); and (c) Object Detection (Wu et al., 2020a) using Faster R-CNN (Zheng et al., 2019; Pearse et al., 2020), Mask R-CNN (Hao et al., 2021; Lumnitz et al., 2021), YOLO (Ampatzidis et al., 2019; Itakura and Hosoi, 2020; Yuan et al., 2022), and RetineNet (Selvaraj et al., 2020; Weinstein et al., 2020b). Image classification-based approach is the earliest method in deep learning based individual tree crown detection methods and proposed in Li et al. (2017), which requires to cooperate the sliding-window technique. Many scholars design new CNN architectures to improve the performance of individual tree crown detection. For example, Dong et al. (2019) propose a progressive cascaded CNN to effectively alleviate wrong detected trees and missing trees in the scene of a complex forest because of unclear canopy contours and abnormal shapes. Their model attains 3.9 ∼ 11% improvement in three study areas located in China, Thailand and America. Dissimilar with the image classification-based approaches that produce one label for a patch of an image, semantic segmentation-based methods aim at generating dense classes for each pixel in the whole image. Some papers propose a modified semantic segmentation model to individual tree crown detection applications. For instance, Zhang et al. (2020) integrate a set of residual U-Nets and a sequence of automatically derived input scales to introduce a new scale sequence residual U-Net-based deep learning algorithm, which is able to complete self-adaption to variations in different kinds of trees, consistently attaining the highest detection accuracy (91.67% on average) compared with the other four state-of-the-art individual tree crown detectionrelated approaches. Object detection-based algorithms consist with the mechanism of the human brain, firstly giving a coarse scan of the whole image and then focusing on areas of interest. They are highly popular in the individual tree crown detection domain with an end-to-end detection framework and high-efficiency, and they contain several correlated stages, such as generating region proposals, CNN based feature extraction, bounding box regression, and classification. For example, Weinstein et al. (2020a) develop a new python package, DeepForest, to detect individual tree crowns through high resolution remote sensing images using object detection based deep learning approach. This package makes the procedures of retraining and utilizing deep learning algorithms more easier for a range of spatial resolutions, sensors and forests. Furthermore, Zheng et al. (2021a) compare different object detection-based algorithms, including Faster R-CNN (Ren et al., 2016), GRID R-CNN (Lu et al., 2019), GA Faster R-CNN (Wang et al., 2019a), Cascade R-CNN (Cai and Vasconcelos, 2019), Libra R-CNN (Pang et al., 2019) and their proposed MOPAD. Experimental results show that MOPAD outperforms other state-of-the-art object detection-based methods by a margin of 8.14 ∼ 21.32% with respect to the average F1 score for multi-class oil palm detection.

However, image classification-based approaches are relatively time-consuming and computationally inefficient due to the adoption of a sliding window approach, particularly when detecting trees of different crown sizes (see Fig. 2). Semantic segmentation-based methods, on the other hand, perform poorly in regions where trees overlap, resulting in the recognition of numerous overlapping or touching trees as a single tree. To construct the final outlines of individual trees, a variety of post-processing processes, such as local maximum detection (Osco et al., 2020), or exclusion of certain objects (Brandt et al., 2020) is frequently required. Generally, the object detection-based algorithms are more efficient and more accurate than existing individual tree crown detection algorithms, eliminating performance reduction caused by difficult terrain and confusion among plant types.

As shown in Table 1, existing coconut tree detection mainly adopted sliding-window technique to achieve coconut tree counting in a picture, which is quite time-consuming. Here we use deep learning object detection-based approaches to recognize coconut trees, which is an end-

to-end detection framework (see Fig. 2). In addition, most existing algorithms use widely available deep learning algorithms without considering their effectiveness in addressing the coarse pixelation problem. However, In this paper, we design a new ITCD methods named COCODET that greatly improves the representation of small tree crowns in deep layers by integrating the information of the candidates in low- and high-level features and providing context semantic information, showing that its effectiveness at coconut tree detection. We think that our novelties in COCODET are quite meaningful in ITCD domain, dealing with the challenges of detecting small and dense tree crowns from remote sensing images using deep learning-based architecture.

3. COCODET: a coconut tree detection approach

Our method is derived from Faster R-CNN (Ren et al., 2016), a basic and popular object detection method. It works by fusing different level features of coconut tree crowns and thereby improving the performance by providing connections between shallow and deep-level semantic features. COCODET has two feature recognition components and a fusion component (Fig. 5):

(1) **An Adaptive Feature Enhancement module** (AFE) for improving the capacity of representation at the highest level of the feature map. Our AFE module has three steps, including multi-scale adaptive pooling, high-level feature enhancement layer and Cross Scale Fusion (CSF). Specifically, improving the feature representation ability at the highest level of the feature map contributes to distinguishing between coconut trees and other tree species or vegetation.

(2) **A Tree-shape Region Proposal Network module** (T-RPN) to find prospects for coconut trees. In contrast to common object detection tasks, we produce region proposals using an end-to-end structure with an aspect ratio of {1: 1} in all levels of features in accordance with the size of a coconut tree crown. Then we generate feature vectors with fixed sizes for all region proposals using a Region of Interest (RoI) pooling layer.

(3) **A Cross Scale Fusion module** (CSF) for integrating multi-scale information to improve the performance of detecting small coconut tree crowns. Our CSF consists of two convolutional layers and a Sigmoid layer to generate a spatial attention map, effecting both after the high-level feature enhancement layer in the AFE module and the RoI pooling layer in the T-RPN module.

By integrating the information of the candidates in low- and high-level features, we greatly improve the detection of small objects such as coconut crowns by provide context semantic information. We believe that these three components in COCODET are really important in the tree crown detection domain, addressing the bottleneck of detecting small and dense tree crowns in remote sensing images using deep learning-based architecture.

3.1. An adaptive feature enhancement (AFE) module

Our backbone is the Residual Network (ResNet) (He et al., 2016), which constructs multiple residual modules in layers, addressing the gradient vanishing problem and degeneration problem in deep neural networks. As Fig. 4 shows, Residual Network allows us to get four distinct scales of feature maps, and we define them as $\{F_1, F_2, F_3, F_4\}$, where F_1 means the feature map at resolution level l. In Feature Pyramid Network (Lin et al., 2017), $\{L_1, L_2, L_3, L_4\}$ represent features with reduced channels, which are lateral connections for $\{P_1, P_2, P_3, P_4\}$.

In a Feature Pyramid Network (FPN), feature maps of $\{P_1, P_2, P_3\}$ is produced through a top-down path and fused with the feature maps at lower levels $\{L_2, L_3, L_4\}$ gradually. However, the highest level P_4 is only produced through itself without other fusion of other level features, suffering from the information loss. As the higher level features perform stronger semantic representations for a larger region, which means they have larger receptive field in images. For example, higher level features are better at distinguishing coconut tree plantations and other similar or complex context (such as other vegetation, bare land, etc.) in a larger area. To this end, we design an Adaptive Feature Enhancement (AFE) module (see Fig. 4(b)) to enhance the representation of the highest level P_4.

Our AFE module has three steps. At first, we generate multiple context features in our AFE module, with different scales of $\{r_1, r_2, r_3\}$ by conducting multi-scale and ratio-invariant adaptive pooling on F_4. Subsequently, each context feature independently undergoes a high-level feature enhancement layer, which unifies the feature channel dimension by a 1×1 convolutional layer. Finally, we design a Cross Scale Fusion (CSF) module (see detailed in Section 3.3) to generate one spatial weight map for each context feature and alleviate the aliasing effect caused by interpolation. CSF combines these feature representations in an adaptive fusion way instead of a direct summation. More details can be found in Section 3.3. To this end, we produce a higher feature level of L_5, which is used to propagated to other lower features.
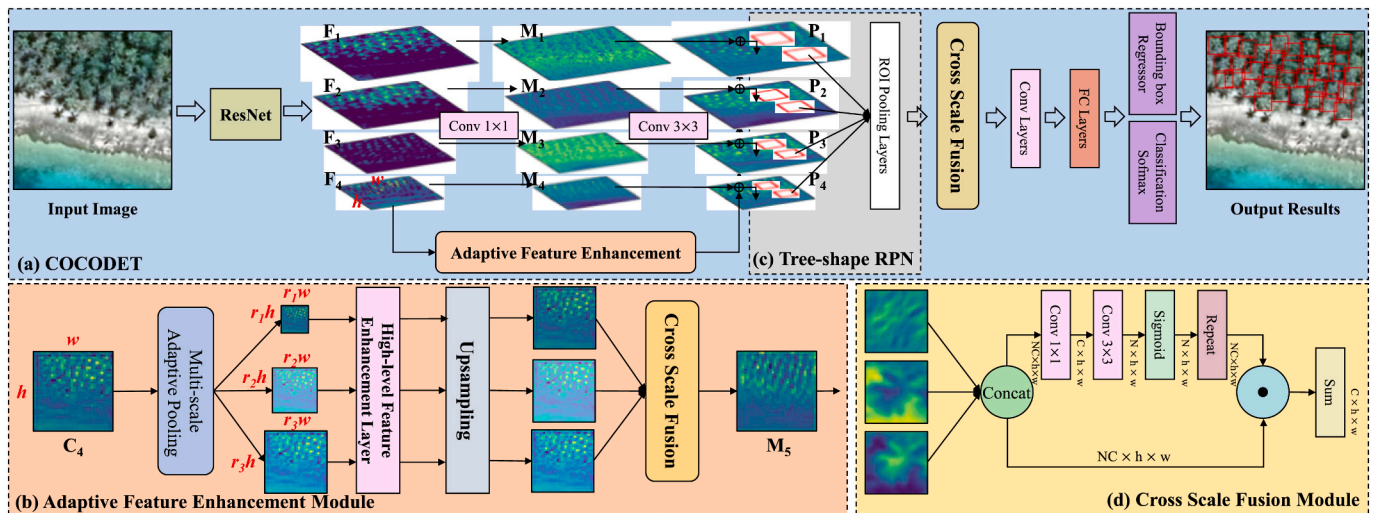

Fig. 4. The framework of the proposed coconut tree detection method - (a) COCODET - includes three modules: (b) An Adaptive Feature Enhancement (AFE) module for improving the capacity of feature representation at the highest level of feature map; (c) a Tree-shape Region Proposal Network (T-RPN) for producing coconut tree candidates; (d) A Cross Scale Fusion (CSF) module for integrating information for multi-scale features, both after the high-level feature enhancement layer in AFE module and the Region of Interest (RoI) pooling layer in T-RPN module.

Therefore, the highest level P$_4$ can be produced through a top-down path and fused with the feature map of L$_5$, acquiring more spatial and context information. Our AFE module improves the feature representation ability at the highest level of feature map, contributing to a better distinction between coconut trees and other tree species or vegetation.

3.2. A Tree-shape Region Proposal Network (T-RPN)

Region Proposal Network (RPN) is widely used in object detection algorithms and applications to generate and filter bounding box candidates, after Faster R-CNN employs this sub-network (Ren et al., 2016), recognizing on the feature maps and instructing the unified network where to look. In the vanilla Faster R-CNN, RPN generates candidates only based on a dense n × n (pixels) sliding window on the last feature map. Here, we use four feature levels (i.e., P1, P2, P3, P4) as the input feature map, and apply the same sliding window to all levels of these features. Following that, using the same approach, Region of Interest (RoI) pooling layer, as the vanilla Faster R-CNN, we use two fully connected (FC) layers for classification and bounding box regression, respectively. Notably, the purpose of the RoI pooling layer is to perform max pooling of inputs of nonuniform sizes to obtain fixed-size feature maps, which is convenient to uniformly process different candidates in the following operators. A fully connected layer multiplies the input by a weight matrix and then adds a bias vector, compiling the image extracted by previous layers to form the final output.

The original anchor sizes in the vanilla Faster R-CNN for the last feature map are {128^2, 256^2, 512^2} and the aspect ratios are {1: 2, 1: 1, 2: 1}. In COCODET, we employ a specific tree-shape anchor size for the level of features after the AFE. With regard to the shape of each coconut tree in the satellite image, we set the anchors sizes of {32^2, 64^2, 128^2, 256^2} pixels on {P$_1$, P$_2$, P$_3$, P$_4$}, respectively. When considering the shape of coconut trees, we just assign {1: 1} at each level as the aspect ratio. Furthermore, because fewer anchors are created, coconut candidate generation strategy in T-RPN speeds up both the training and reference processes.

3.3. A Cross Scale Fusion (CSF) module

After T-RPN (see Sec. 3.2), we generate a series coconut tree crown candidates from four different feature levels of the same size. Although the original FPN (Lin et al., 2017) (see Fig. 4(a)) fused low-level and highlevel features {P$_1$, P$_2$, P$_3$, P$_4$}, it still focused on their own level features. If we integrate the information of the candidates in low-level features (such as P1) with the information of the candidates in high-level features (such as P$_4$), it significantly benefits the detection of small objects such as coconut crowns with more abundant context semantic information. To deal with this issue, the Path Aggregation Network (PANet) (Liu et al., 2018) adopts an adaptive feature pooling to refine the proposals from all pyramid levels' features, and utilize Fully Connected (FC) layers with a maximum or a summation. On the other hand, other studies (Hu et al., 2018; Guo et al., 2020) adopts global max pooling or global average pooling before fusing candidates from multi-level features. However, these methods inevitably to suffer from time-consuming FC layers and information-loss pooling layers.

Therefore, we design a Cross Scale Fusion (CSF) module, fusing multi-scale candidates (acquired from Sec. 3.2) from different level features without parameters-increasing FC layers (Liu et al., 2018). Our CSF first concatenates high- and low-level features, followed by two convolutional layers. After that, it undergoes a sigmoid layer to generate spatial weight maps for Region of Interest (RoI) outputs from multi-scale levels. The sigmoid layer applies a sigmoid function to the input such that the output is bounded, which is similar to the perceptron and much smoother than the step function in the perceptron. Finally, the spatial weight maps conduct a Hadamard product with concatenated candidates from different levels. Notably, the Hadamard product is a binary operation that takes two matrices of the same dimensions and produces another matrix of the same dimension as the operands. To this end, the CSF learns to produce more representative candidates from multi-scale feature levels, especially improving the performance of detecting small coconut tree crowns by connecting the shallow and deep level context semantic features. Furthermore, this CSF module is also a component in the AFE module (see Sec. 3.1) to adaptively fuse multi-scale features generated from C$_4$ and acquire an enhanced feature M5 (see Fig. 4(c)).

Overall, the final loss function of our COCODET can be formulated as Eq. (1), including classification loss (L_{cls}) and localization loss (L_{loc}).

$$L_{\mathrm{COCODET}} = \sum_{P=1}^{4} \left(L_{cls,P}(\boldsymbol{p}, t^*) + \beta[t^* > 0]L_{loc,P}(\boldsymbol{d}, b^*) \right) \tag{1}$$

in which β is the trade-off weight to balance the classification and localization of the bounding-box loss. We utilize softmax cross-entropy loss for classification loss and Smooth L$_1$ loss for bounding-box regression loss (Ren et al., 2016). t^* and b^* are the true values of class labels and bounding-boxes, respectively. $\boldsymbol{p}$ and $\boldsymbol{d}$ are the classification and regression predictions for the final pyramid layers ({P$_1$, P$_2$, P$_3$, P$_4$}), respectively.

3.4. Large-scale coconut tree detection process

We apply our proposed COCODET on the coconut tree crown detection in four remote atolls in the Acteon Group of the Pacific Ocean for large-scale testing. As we train the model using sub-images of 512 × 512 pixels, we crop the large-scale image into small patches to match the training model and achieve high-speed prediction when implementing the large-scale test. In addition, we utilize an overlapping strategy for largescale applications. Each of the two neighboring sub-images own an overlapping area of 100 × 100 pixels to make sure every coconut tree in images is complete and no corners are left ignored, rather than directly cropping into several 512 × 512 sub-images. To obtain the final detection results, we conduct an Intersection-of-Union (IoU) based merging procedure after each patch's coconut tree detection. IoU based merging procedure overcomes the mis-detection, incorrect detection of coconut tree crowns in large-scale applications, and it prevents any duplication problems. Furthermore, we draw the land contours for these isolated atolls and drop the discovered coconuts into the ocean automatically.

4. Experiments and evaluation

4.1. Site and data description

4.1.1. Site description

Our study area is the Acteon Group (*Groupe Act'eon*) in French Polynesia, which is about 1400 km east-southeast from Tahiti. They form part of the Windward group of Society Islands, and are isolated and uninhabited atolls. The first European to sight the Acteon Group was Pedro Fernández de Quirós on 5 February 1605. He described the group as "four atolls crowned by coconut palms" (Nowell, 1968). They were more thoroughly explored by Thomas Ebrill, captain of the Tahitian trading vessel Amphitrite, in 1833.

Two of the four atolls in this group - Tenararo and Vahanga - are recognized as a Key Biodiversity Area and proposed as an Important Bird Area (Griffiths et al., 2011). Threatened endemics include two endangered birds identified as priorities for species-specific investment: the Polynesian ground dove (*Gallicolumba erythroptera*) and the Tuamotu sandpiper (*Prosobonia cancellata*) (Griffiths et al., 2008; Curlew, 2014). Other native threatened species present in the Ackeon Group include atoll fruit-dove (*Ptilinopus coralensis*), Murphy's petrel (*Pterodroma ultima*), bristle-thighed curlew (*Numenius tahitiensis*) and green turtle (*Chelonia mydas*) van der Vliet and Ghestemme (2013); Pierce et al. (2015); Veitch et al. (2019).

The Acteon Group have four main atolls: Tenararo, Vahanga, Tenarunga and Matureivavao (see Table 2). Tenararo is the smallest

Table 2
Summary statistics four atoll comprising the Acteon Group (from (Griffiths et al., 2008)).

Index	Tenararo	Vahanga	Tenarunga	Matureivavao
Total area (including reef and lagoon area; ha)	700	1258	1349	2862
Land area (including vegetation area; ha)	272	382	425	396
Vegetation area (percentage of total land area; ha)	106 (39%)	115 (30%)	136 (32%)	55 (14%)
Distance from the Vahanga (km)	7	–	8	17

atoll in the Acteon with only 700 ha of total area and there is no entrance to the lagoon. This atoll has a landing place on its northwest side between the small boulders which encumber the reef (Moulin, 1866). Vahanga is a circular atoll with a diameter of 3.6 km and a land area of 382 ha (including a 1258 ha lagoon). It is a low atoll with a landing place on the northwest side of the island near a white house, but there is no access to the lagoon (DATA, 2006). Tenarunga is located 8 km east of Vahanga, with a land area of 425 ha and a total area of 1349 ha (lagoon inclusive). There are some buildings and a dock located on the northeast side of this island, indicating former or seasonal habitation (Dahl, 1986; Quanchi and Robson, 2005). Matureivavao is the largest atoll, with a land area of 396 ha and a lagoon area of 2466 ha (Young, 1899).

Coconut dominate the islands, with other vegetation types including grasslands, flooded vegetation and shrubland occupying only 15% of the land (see Karra et al. (2021)). As natural components of the vegetation, coconuts can be beneficial for wildlife: fruits and insect larvae in rotting coconut fruits are important foods for Tutururu; tall coconut trees provide refuge for birds and may afford some protection against tropical cyclones (Blanvillain et al., 2002). On the other hand, the common practise of clearing native undergrowth beneath mature coconut stands depletes the Tuamotu Sandpiper habitat (Pierce and Blanvillain, 2004) threatening this and other bird species. Another threat to wildlife are the mammals introduced to all the atolls except Tenararo (Blanvillain, 2000; Blanvillain et al., 2002), including Pacific and Black rats, and some cats in Tenarunga (Brooke et al., 2007).

4.1.2. Data description

Four DigitalGlobe satellite photos were obtained from Google Earth with 0.6 m spatial resolution and three spectral bands (red, green and
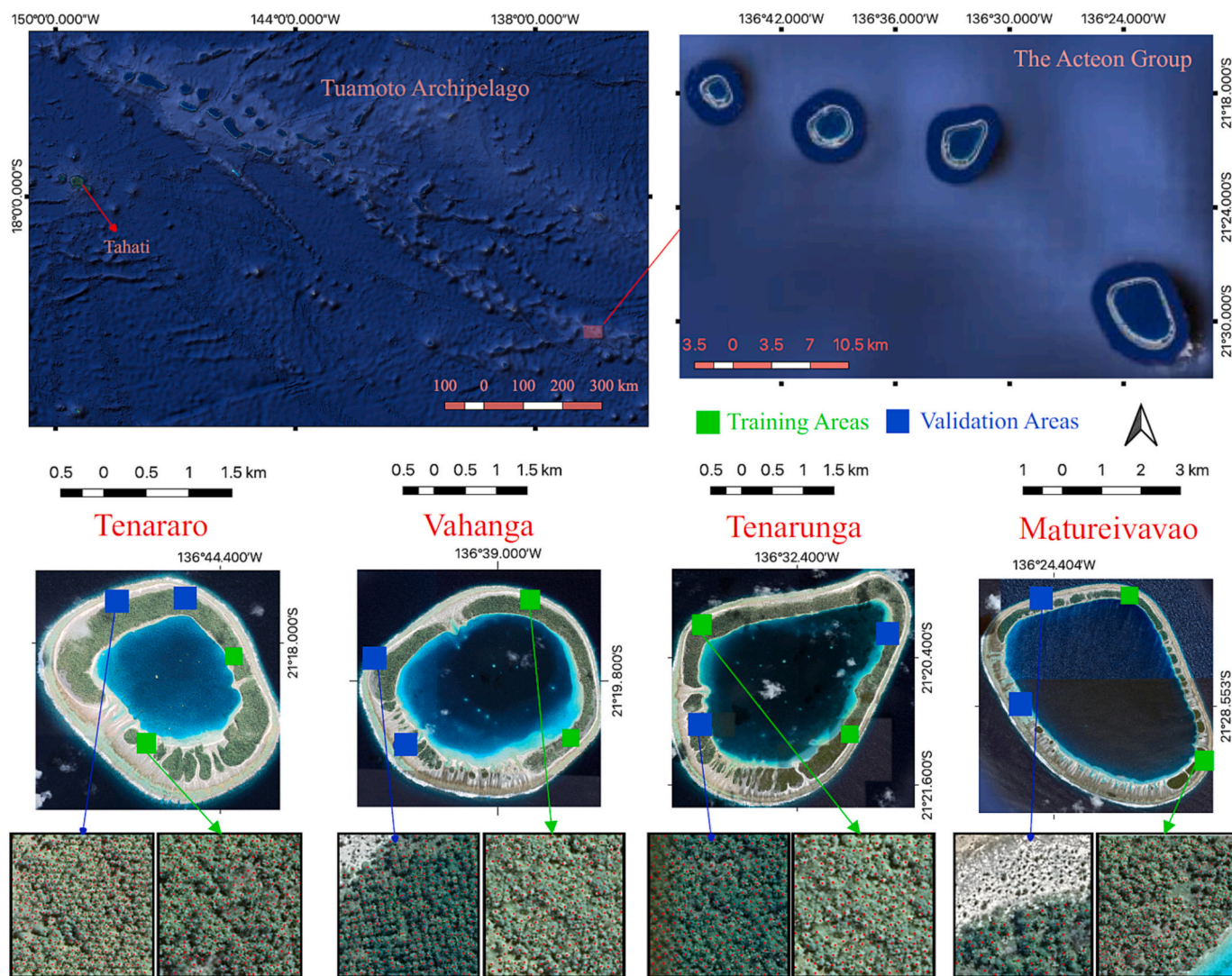

Fig. 5. The location of the Acteon Group and its four atolls, named Tenararo, Vahanga, Tenarunga and Matureivavao. We also point out our training areas (green squares) and validation areas (blue squares) where we have manually annotated all coconut trees (red points). (For interpretation of the references to colour in this figure legend, the reader is referred to the web version of this article.)

blue). We train our model using eight training regions (denoted by the green squares, two zones for each atoll, see Fig. 5) and validate the model using eight validation regions (denoted by blue rectangles, two zones for each atoll, see Fig. 5) during training procedures. We report the model's performance in the test region, which is the whole area of four atolls in the Actoen Group. Notably, the area of the training set or validation set accounted for <1.7% of the total area of the test region. Although the training set and validation set are included in the large-scale test set, it is reasonable and suitable to report our results in the test region, which is the same as other large-scale deep learning applications (Brandt et al., 2020).

To this end, we chose two training zones (the green squares in Fig. 5) for each atoll with 3000 × 3000 pixels, and two regions as validation regions (the blue squares in Fig. 5) with 3000 × 3000 pixels. All coconut trees in our training and validation regions were labeled manually (red points in the last row of Fig. 5). We generated a training dataset of 2000 photos by randomly cropping each training image with 512 × 512 pixels and feeding it into deep neural networks (each training region generates 50 images and we adopt four data augmentation strategies including horizontal flipping, vertical flipping, random cropping and noise addition). We also arbitrarily trimmed the validation dataset with 512 × 512 pixels, and there were 200 validation photos in total (each validation generated 50 images). For the test dataset, we adopt an overlapping partition approach for the whole satellite image shown in Fig. 5 (see detailed information in Section 3.4).

4.2. Performance of COCODET

The performance of COCODET for coconut tree crown detection is tested using field observations (Section 4.2.1). We show the detection results of COCODET in Section 4.2.2. Providing deep insights, we conduct comprehensive ablation studies and compare our results with other state-of-the-art (SOTA) object detection algorithms in Section 4.2.3 and Section 4.2.4.

4.2.1. Settings and evaluation

We employ the MMdetection as our experiment conduction deep learning framework (Chen et al., 2019), and we predefine the hyper-parameter (introduced in Eq. 1) as 1 throughout all experiments (Ren et al., 2016). We use GeForce RTX 2080 Ti to train our model and the training epoch is 24. The backbone we choose for all the algorithms in the comparative work is ResNet-101 for a fair comparison. Stochastic Gradient Descent (SGD) is chosen as our optimizer and we also use a momentum of 0.9. The initial learning rate is set as 0.01 and it decreases by a ratio of 0.1 after the 12th and 16th epoch, respectively. The values of {r1, r2, r3} are set as {0.1, 0.2, 0.3}. The other hyper-parameters in our experiments are the same with the default settings in MMdetection.

Precision, recall, and F1 score are included in the assessment metrics. Precision measures the model's ability to properly recognize coconut trees, whereas recall measures its ability to locate ground-truth coconut plants. The F1 score represents the model's overall performance. Aforementioned metric can be formulated from True Positives (TP), False Positives (FP) and False Negatives (FN) as Eq. 2. TP means how many coconut trees that are detected correctly; FP means the number of others recognized as coconut trees by mistake; FN means how many coconut trees that are mis-detected. If the IoU metric value between the detected tree and the corresponding ground truth is equal to or >0.7 (see Sec. 4.2.4), the coconut tree may be considered as a correctly detected target.

$$precision = \frac{TP}{TP + FP}$$

$$recall = \frac{TP}{TP + FN} \quad (2)$$

$$F1 \ score = \frac{2 \times precision \times recall}{precision + recall}$$

4.2.2. Results

We used our proposed COCOnut tree DETection algorithm (COCO-DET) to provide a wall-to-wall map of coconut trees across the four abandoned atolls (see Sec. 3). We selected training regions on each atoll with a total area of 36 ha and test the whole atoll to evaluate the accuracy of coconut tree detection. Table 3 lists the six indices (i.e., TP, FP, FN, precision, recall and F1 score) for four remote atolls in the Acteon Group. COCODET achieves an average F1 score of 86.46%, with 82.56 ~ 89.19%. The performance of the Tenararo is better than that of other atolls, with 0.81 ~ 8.27% increase in the F1 score. The explanation for this might be that Tenararo has the most coconut trees per unit of land area, which helps to minimize misunderstandings between coconut trees and other land cover categories (see Table 2). Fig. 6 illustrates some cases of FP (on the left) and FN (on the right). We can observe that tree shadows or other vegetation might be recognized as coconut trees falsely. Also, some FPs may results from the overlapping between two coconut tree crowns or dissatisfaction with the specific IoU metric (see Fig. 6(a)). As for FN, it is primarily contributed from covering by other tree crowns or vegetation, which is owing to the low quality of satellite images or the small size of the coconut tree crown (see Fig. 6(b)).

4.2.3. Results comparison between our proposed COCODET and other State-Of-The-Art (SOTA)

Comparison of our method with seven different cutting-edge object detection methods, including RepPoints (Yang et al., 2019), Faster R-CNN (Ren et al., 2016), Libra Faster R-CNN (Pang et al., 2019), Guided Anchoring (GA) Faster R-CNN (Wang et al., 2019a), RetinaNet (Lin et al., 2018), Cascade R-CNN (Cai and Vasconcelos, 2019) and Grid R-CNN (Lu et al., 2019), MOPAD (Zheng et al., 2021a), Sparse R-CNN (Sun et al., 2021) and PTDM (Yuan et al., 2022). Faster R-CNN (Ren et al., 2016) is a fundamental object detection approach of our proposed COCODET and has been used in various tree crown detection studies (Pearse et al., 2020; Zheng et al., 2021a). RepPoints (Yang et al., 2019) learns to arrange ground truth localization and recognition targets automatically through bounding an object's spatial extent. Cascade R-CNN (Cai and Vasconcelos, 2019) contains a series of detectors to ensure high-quality object detection with adaptive IoU thresholds. GA Faster R-CNN (Wang et al., 2019a) utilizes semantic features to predict both the locations and the scales and aspect ratios in the RPN, which is introduced in Sec. 3.2. RetinaNet (Lin et al., 2018) concentrates training on a sparse set of hard examples and avoid a large quantity of easy negatives from overwhelming the detector during training. Libra Faster R-CNN (Pang et al., 2019) addresses three different levels of imbalance, including objective level, feature level and sample level through balanced L1 Loss, balanced feature pyramid, and IoU-balanced sampling, respectively. Grid R-CNN (Lu et al., 2019) mainly adopts a grid guided localization scheme to attain outstanding object detection results. MOPAD (Zheng et al., 2021a) combines a Refined Pyramid Feature (RPF) module and a hybrid class-balanced loss module to achieve satisfying observation of the growing status of individual tree crowns.

Table 3
The precision, recall and F1 score for four atolls using deep learning based tree detection methods.

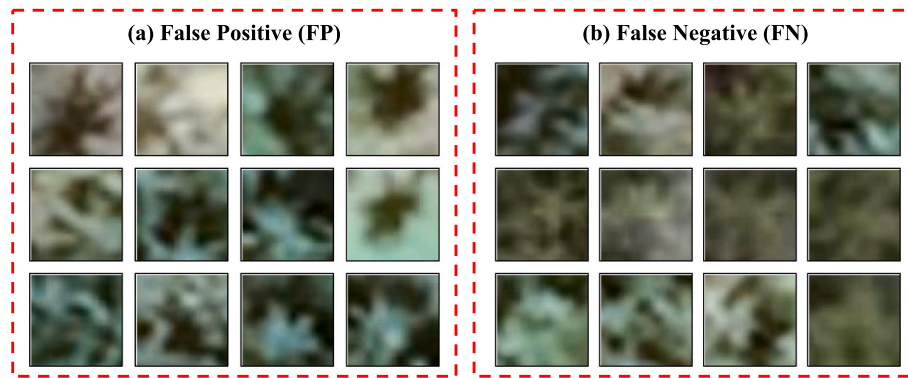| Index	Tenararo	Vahanga	Tenarunga	Matureivavao
TP	32,313	19,753	25,789	26,428
FP	3884	3274	5583	3213
FN	3952	3403	5316	3619
Precision	89.27%	85.78%	82.20%	89.16%
Recall	89.10%	85.30%	82.91%	87.96%
F1-score	89.19%	85.54%	82.56%	88.55%
Average F1 score	86.46%			

Fig. 6. Failure cases for FP and FN of coconut tree detection.

Sparse R-CNN (Sun et al., 2021) completely avoids all efforts related to object candidates design and many-to-one label assignment by eliminating handdesigned object candidates for learnable proposals. PTDM (Yuan et al., 2022) proposes a tree detection method that introduces the attention mechanism and a Ghost module into the lightweight model network, as well as a feature-fusion module to improve the feature-extraction ability.

We show coconut tree crown detection results for these four remote atolls in Table 4. Our proposed COCODET achieves the average F1 score of 86.46% for coconut tree crown detection, with improvements of 4.33 ~ 12.02% compared to other SOTA object detection algorithms. In general, one-stage object detectors (RetinaNet and RepPoints) perform worse than two-stage object detectors, which is in line with the general trend (Zhao et al., 2019; Oksuz et al., 2020). Especially, we can find out that our COCODET has significantly greater accuracy for coconut tree crown detection in the Vahanga, with 4.65% ~ 11.49% improvement. Although Faster R-CNN performs better than two one-stage object detectors (RetinaNet and RepPoints), with improvements of 5.33% and 0.86%, respectively, with an average F1 score of 79.77%, it is showing indications of degradation. Libra R-CNN, Cascade R-CNN, GA Faster R-CNN and Grid R-CNN achieve some improvements compared to Faster R-CNN with 0.25 ~ 1.75% gain. Figs. 7-10 display the detection results of aforementioned object detection methods, which demonstrate the best results of our proposed COCODET compared with other SOTA algorithms. The green points, red squares and yellow circles represent TPs, FPs and FNs, respectively. COCODET identifies much fewer confusions with other vegetation, shadows, and so on, and has fewer missing coconut trees. More COCODET results and comparative results can be found in Figs. A.23 ~ A.26 in Appendix A.

4.2.4. Ablation studies for COCODET

In this section, we initially analyze how different depths of ResNet influence the model performance and anchor generation methods. Then, considerable ablation tests are performed, assessing the Adaptive Feature Enhancement (AFE) and the Cross Scale Fusion (CSF). These ablation tests highlight the effectiveness of individual component and add deeper understanding to our propose COCODET.

Comparisons among different CNN backbone networks, the anchor generation ways and the threshold of confidence. The effectiveness of different depths of ResNet and ResNeXt is shown in the Table 5 (Xie et al., 2017), including 50, 101 and 152 layers. ResNeXt (Xie et al., 2017) is constructed through repeating a building block that aggregates a series of transformations with the same topology, only setting a few hyper-parameters. ResNet-101 has the greatest average F1 score of 86.46% for coconut tree crown detection and the highest F1 score for the Vahanga and the Matureivavao according to experiment results. ResNeXt-101 and ResNet-152 achieve the highest accuracy for the Tenarunga and the Tenararo, respectively. As a result, we chose ResNet-101 as the foundation for our proposed COCODET. To assess the methods of anchor formation, we conduct ablation tests on various aspect ratios and anchor sizes. As shown in Table 6, the scale setting $\{32^2, 64^2, 128^2, 256^2\}$ improves the average F1 score compared to $\{64^2, 128^2, 256^2\}$. On the other hand, although the ratios of $\{1: 2, 1: 1, 2: 1\}$ (the last row in Table 6) slightly outperform than our tree-shape ratios of $\{1: 1\}$ under scale setting of $\{32^2, 64^2, 128^2, 256^2\}$, we maintain the ratio setting of $\{1: 1\}$ since this ratio is more appropriate and flexible because of the forms of coconut tree tops and the acceleration with considerably less creation of candidates throughout the training and reference time. Furthermore, we analyze the effect of the confidence threshold as shown in Fig. 11, which means that we consider the detected bounding box whose probability of classification is larger than the confidence as a coconut tree. Although different atolls achieve the highest F1 score under different confidence thresholds (0.6 ~ 0.8), the average F1 score attains the peak value at a confidence of 0.7. Therefore, we select 0.7 as our confidence threshold in this paper.

Effectiveness for the Adaptive Feature Enhancement (AFE). The ablation studies of AFE are shown in Table 7. We firstly evaluate three different kinds of pooling strategies, including Global Max Pooling (GMP) (Lin et al., 2013), Global Average Pooling (GAP) (Lin et al., 2013) and our proposed Multi-scale Adaptive Pooling (MAP). In this way, we

Table 4

Comparisons (F1 score) among different object detection-based deep learning methods for coconut tree detection in the Acteon Group.

| Method	Tenararo	Vahanga	Tenarunga	Matureivavao	Average
Faster R-CNN (Ren et al., 2016)	85.38%	77.95%	73.36%	82.41%	79.77%
RetinaNet (Lin et al., 2018)	80.12%	74.05%	67.44%	76.19%	74.44%
GRID R-CNN (Lu et al., 2019)	84.20%	80.72%	77.24%	83.93%	81.52%
GA Faster R-CNN (Wang et al., 2019a)	86.66%	77.42%	73.59%	82.40%	80.02%
Cascade R-CNN (Cai and Vasconcelos, 2019)	83.45%	80.89%	76.89%	83.69%	81.23%
Libra R-CNN (Pang et al., 2019)	83.91%	79.19%	74.84%	82.87%	80.20%
RepPoints (Yang et al., 2019)	83.33%	79.38%	71.31%	81.62%	78.91%
MOPAD (Zheng et al., 2021a)	84.23%	79.48%	77.88%	84.65%	81.56%
Sparse R-CNN (Sun et al., 2021)	84.82%	79.71%	79.81%	84.16%	82.13%
PTDM (Yuan et al., 2022)	83.45%	80.08%	80.07%	84.04%	81.19%
COCODET (ours)	**89.19%**	**85.54%**	**82.56%**	**88.55%**	**86.46%**
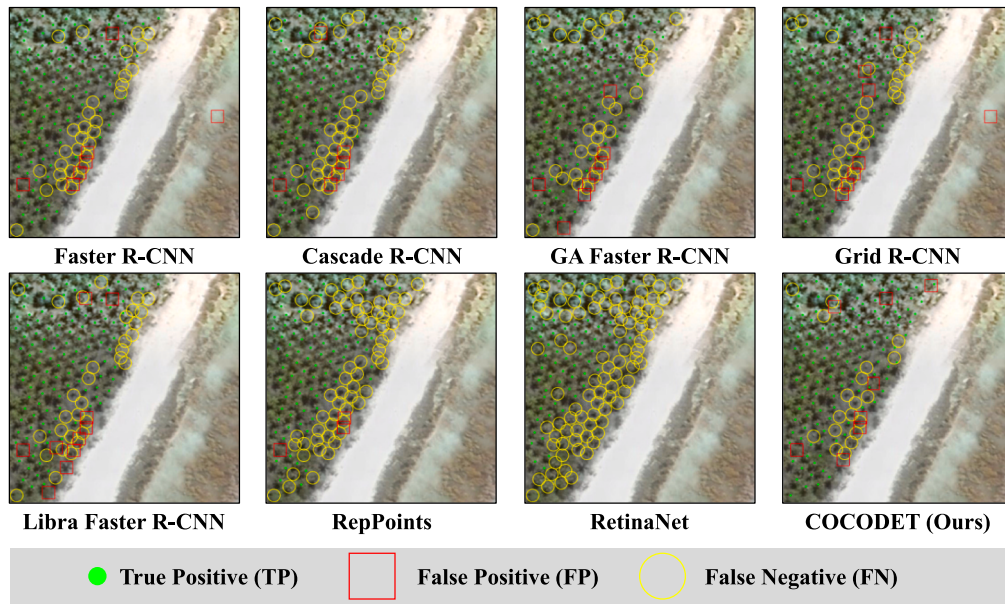
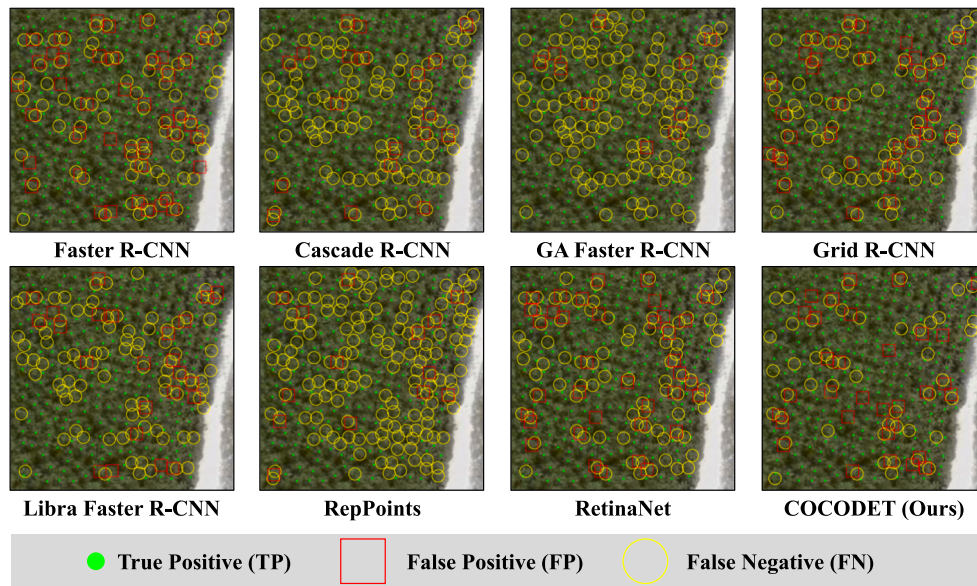**Fig. 7.** Coconut tree crown detection results for Region 1 in the Tenararo.

Fig. 8. Coconut tree crown detection results for Region 1 in the Vahanga.

adopt summation as the base fusion type instead of the Cross Scale Fusion (CSF). We maintain other settings as same as Faster R-CNN (Ren et al., 2016) and our T-RPN (Sec. 3.2). We can observe that our MAP is the best pooling type among these three pooling strategies, attaining 0.18 ∼ 0.93% gain. It seems that our MAP holds stronger capacity of representation, preventing less information loss from the pooling strategy. As for fusion type, we compare summation, Pyramid Scene Parsing (PSP) (Zhao et al., 2017) and our proposed CSF. PSP exploits the capability of global context information through pyramid pooling module, attaining 1.47% gain with respect of average F1 score compared to summation. Furthermore, adopting our CSF fusing scheme, the average F1 score further improve 1.73% compared to PSP (Zhao et al., 2017), indicating that our CSF is expert in detecting small coconut tree crowns through connecting the shallow and deep level context semantic features. Some visualization comparisons can be found in Fig. 12.

Effectiveness for the Cross Scale Fusion (CSF). Our CSF appears twice in COCODET, first in the AFE module (see Fig. 4(c) in Sec. 3.1),

and then after T-RPN (see Fig. 4(d) in Sec. 3.3). Sec. 4.2.4 demonstrates that CSF performs higher detection accuracy compared to other fusion types in the AFE module. Without using the CSF strategy, the original Faster R-CNN directly undergoes convolutional layers and FC layers. The last row of Table 7 shows that utilizing our CSF after RoI pooling layers improves the detection results with a 1.48% gain of average F1 score and with 0.78%, 1.99%, 1.64% and 1.53% improvement for the four atolls, respectively. Also, we can observe that in Fig. 12, there are much less false positives (other objects detected as coconut trees) and less false negatives (missing coconut trees) after adopting CSF strategy, either in AFE module or after T-RPN module.

Sensitive analysis for hyperparameters tuning. We compare the performances under different hyperparameters, such as the trade-off weight β in Eq. 1 (see Fig. 13(a)), the optimizer (see Fig. 13(b)), the momentum (see Fig. 13(c)) and the learning rate (see Fig. 13(d)). Therefore, according to Fig. 13, Stochastic Gradient Descent (SGD) is chosen as the optimizer, and we use the momentum of 0.9 and the initial
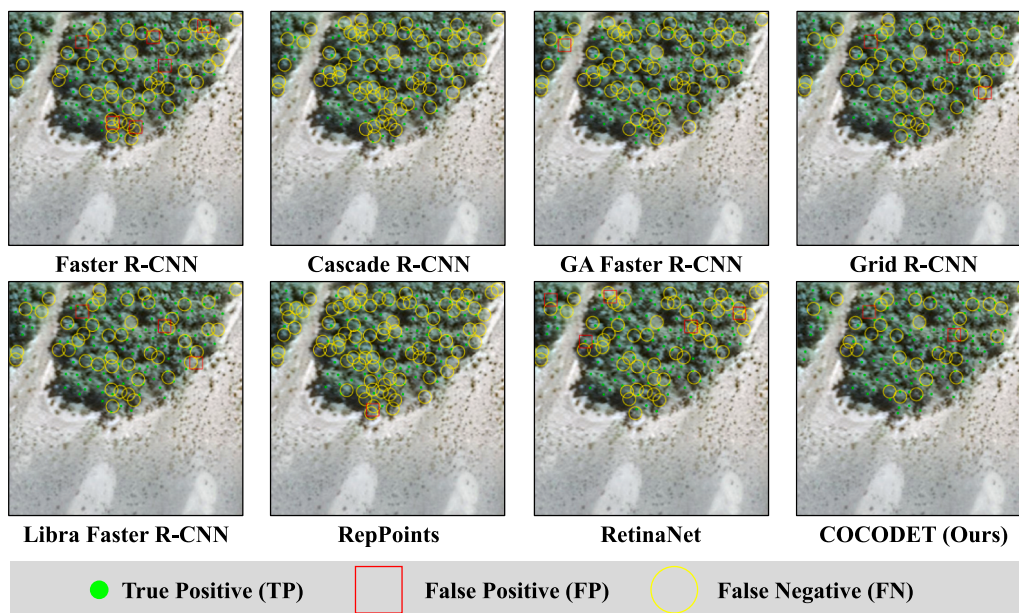
Fig. 9. Coconut tree crown detection results for Region 1 in the Tenarunga.
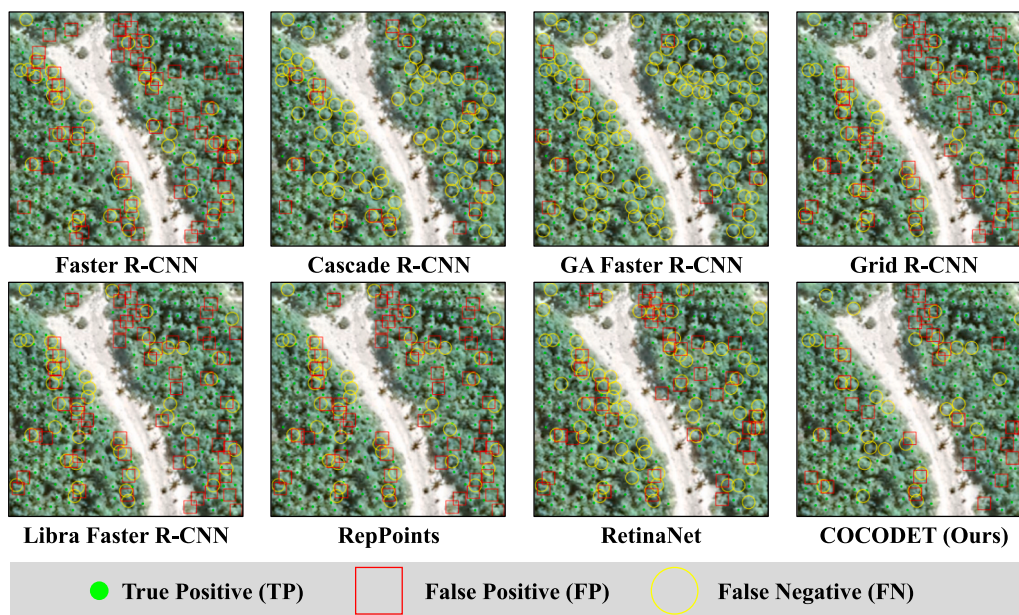

Fig. 10. Coconut tree crown detection results for Region 1 in the Matureivavao.

learning rate of 0.01. The trade-off weight β is used to balance the classification and localization of bounding-box loss, and β = 1.0 achieves the highest coconut detection performance.

We also display the training loss and the validation loss in Fig. 14. Generally, learning rate decay is a common technique to help the network converge to a local minimum and avoid oscillation (Ng, 2017). As shown in Fig. 14, when we decrease the learning rate by a factor of 0.1 after the 12th and 16th epoch, we can find that the validation loss has a clear decrease around the 12th epoch and 16th epoch. Also, decreasing the learning rate makes both the validation and training loss curve less oscillating, helping to better optimize and generalize the model.

5. Discussion

In the following, we first discuss the relationship between coconut tree detection performance and other factors, including different land cover types, different elevation values and different crown sizes in Sec. 5.1. And then, we discuss the connections between coconut tree distribution and ecological function of islands in the Acteon Group (Sec. 5.2). Then, we provide more specific information on how the coconut plantation can wildlife biodiversity, including positive and negative impacts in Sec. 5.3. After that, we examine the transferability of COCODET for ITCD in general in Sec. 5.4. Finally, we discuss the potential applications of COCODET in Sec. 5.5.
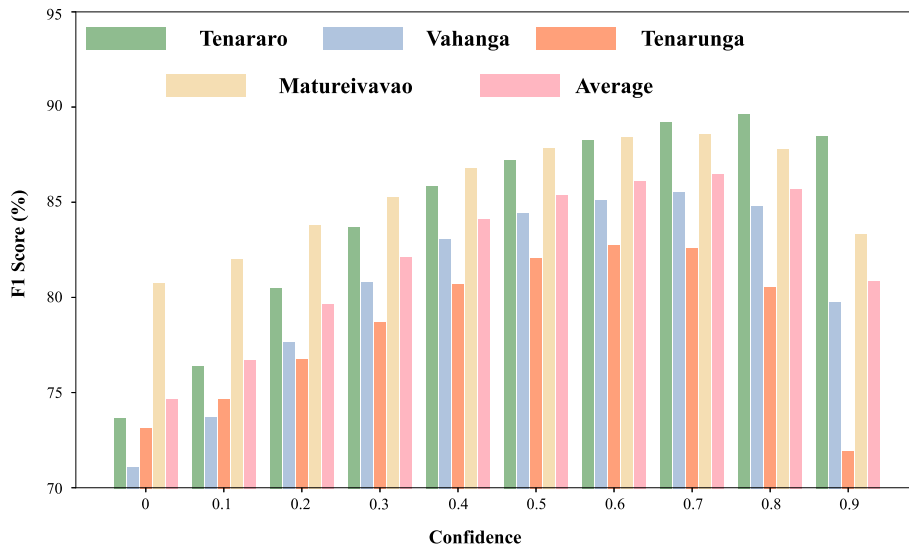
Fig. 11. The F1 scores of coconut tree detection under different confidence threshold.

Table 5

The F1 scores of different depth of ResNet and ResNeXt for our COCODET.

Method	Tenararo	Vahanga	Tenarunga	Matureivavao	Average
ResNet-50	85.19%	80.46%	76.17%	84.64%	81.62%
ResNeXt-50	85.35%	80.02%	76.78%	85.08%	81.81%
ResNet-101	89.19%	**85.54%**	82.56%	**88.55%**	**86.46%**
ResNeXt-101	88.92%	84.03%	**83.52%**	87.00%	85.87%
ResNet-152	**90.71%**	84.79%	80.64%	86.56%	85.68%
ResNeXt-152	84.61%	80.79%	79.58%	85.03%	82.74%

5.1. Relationships between coconut tree detection performance and other factors

5.1.1. Relationship between coconut tree detection performance and land cover types

As for the relationship between detection performance and different land cover types, we use ESRI land cover mapping with a 10 m resolution (see Fig. 15) (Karra et al., 2021) and display the F1 score and the land cover types for these four atolls in Fig. 16. ESRI land cover results have some obvious misclassification (such as "Snow/Ice"), which can be seen in Fig. 15. We can find that the detection performance achieves highest F1 score on the land cover of "Trees", and achieves lowest F1 score on the land cover of "Snow/Ice" or "Flood vegetation", which indicates there exists more confusions on other land cover types, causing more false positives for other objects detected as coconut trees.

Land cover mapping is quite essential for building assessment of the ecological environment of the Acteon Group. To this end, the accurate monitoring of coconut trees and land cover changes in these remote atolls from remote sensing images is quite essential to know the development of the expansion of these loopholes and the growing status of

coconut trees. In addition, tree species classification is also quite important for these four remote atolls from an environmental perspective. As introduced in Sec. 4.1.1, coconut palm trees have dominated the Acteon Group for over 500 years, where the ecosystem is really simple. To this end, recognizing other tree species in these atolls can help us to understand the development of ecological evolution. Also, other tree species in between the rows of coconut plantations can enrich the plant diversity, enhance ecological resistance and increase the food product for endangered bird species (such as Pisonia and Achyranthes) (Lees et al., 2022). Therefore, both land cover types and tree species classification are crucial for these four remote atolls, reflecting the relationship between coconut palms and other plant species, and know about the overall environmental and ecological conditions of the atolls.

Table 7

Comparisons among different strategies, including Faster R-CNN (the baseline) (Ren et al., 2016), MAP, PSP (Zhao et al., 2017), AFE and CSF.

Method	Tenararo	Vahanga	Tenarunga	Matureivavao	Average
Faster R-CNN	85.38%	77.95%	73.36%	82.41%	79.77%
+ **GMP**[*]	84.30%	79.77%	76.15%	83.18%	80.85%
+ **GAP**[♯]	84.95%	**80.89%**	76.89%	83.69%	81.60%
+ **MAP**[†]	**85.38%**	80.85%	**77.03%**	**83.85%**	**81.78%**
+ **MAP + PSP**[♭]	86.56%	82.52%	78.55%	85.38%	83.25%
+ **MAP + CSF (AFE)**	**88.41%**	**83.55%**	**80.92%**	**87.02%**	**84.98%**
+ **AFE + CSF**	**89.19%**	**85.54%**	**82.56%**	**88.55%**	**86.46%**

*GMP denotes Global Max Pooling. ♯GAP denotes Global Average Pooling. †MAP denotes Multi-scale Adaptive Pooling. ♭PSP denotes Pyramid Scene Parsing.

Table 6

The F1 scores of ablation studies of different anchor sizes and aspect ratios.

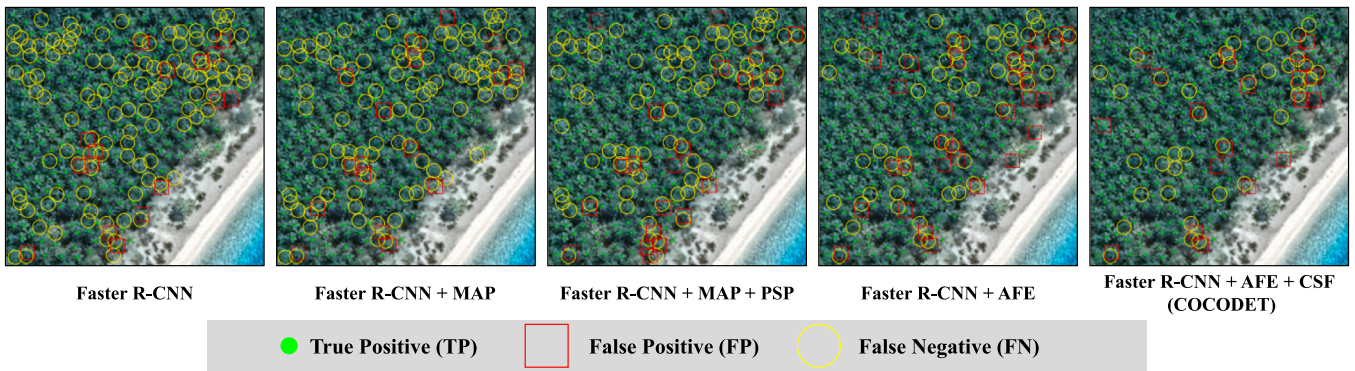| Ratios	Scale	Tenararo	Vahanga	Tenarunga	Matureivavao	Average
{1: 1}	{64^2, 128^2, 256^2}	86.01%	83.20%	80.85%	86.63%	84.17%
{1: 2, 1: 1, 2: 1}	{64^2, 128^2, 256^2}	87.05%	83.91%	81.51%	87.18%	84.91%
{1: 1}	{32^2, 64^2, 128^2, 256^2}	89.19%	**85.54%**	82.56%	**88.55%**	86.46%
{1: 2, 1: 1, 2: 1}	{32^2, 64^2, 128^2, 256^2}	**89.63%**	85.13%	**82.73%**	88.40%	**86.47%**

Fig. 12. Comparisons among different strategies, including Faster R-CNN (the baseline) (Ren et al., 2016), MAP, PSP (Zhao et al., 2017), AFE and CSF.
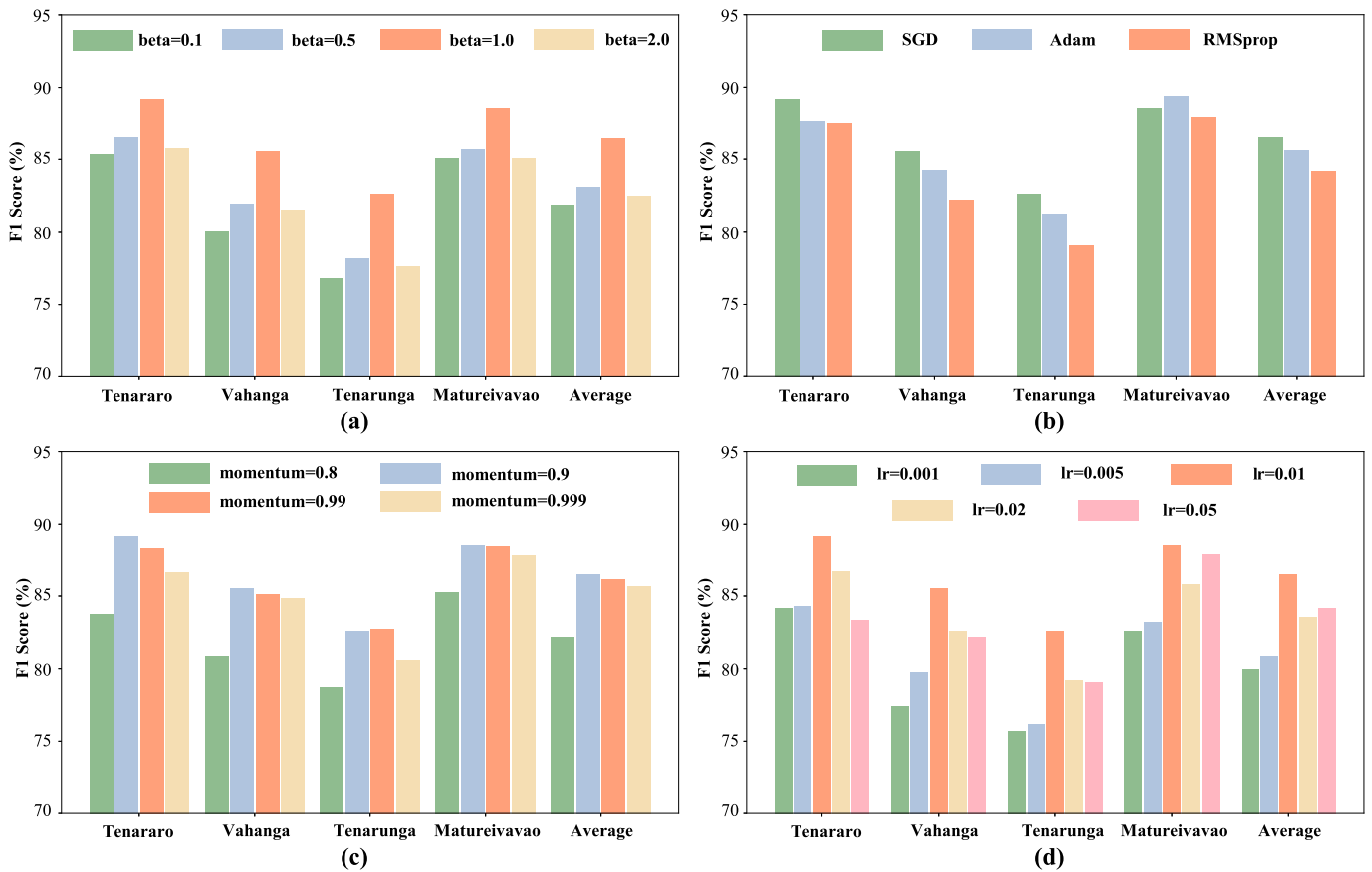

Fig. 13. (a) The F1 scores of different trade-off weight β in Eq. (1) for our COCODET. (b) The F1 scores of different optimizers for our COCODET. (c) The F1 scores of different momentum for our COCODET. (d) The F1 scores of different learning rates for our COCODET.

5.1.2. Relationship between coconut tree detection performance and the crown size

Here, we discuss how tree crown sizes influence detection results in these four remote atolls. We classify the tree crown sizes into three categories: (a) small tree crown size (diameter < 8 m); (b) general tree crown size (8 m $\leq$ diameter < 13 m); and (c) large tree crown size (diameter $\geq$ 13 m). Table 8 lists the precisions of coconut detection under different sizes of tree crowns using our proposed COCODET in the Acteon Group. We calculate the precision according to Eq. (2) using TP and FP (see their definitions in Eq. (2) in Sec. 4.2.1). 515 We can observe that most of the tree crowns' diameter are 8 ~ 13 m and their average precision is 87.53%, which is much higher than the precisions of the small tree crown size and the large tree crown size. Although our COCODET is better at detecting small objects in remote sensing images

than other object detection-based algorithms, it suffers serious deterioration of precision towards smaller objects (when the diameter of coconut tree <8 m). The another reason of low performance for coconut trees with small tree crown sizes and large tree crown sizes maybe that our training dataset is lack of coconut trees with small tree crown sizes and large tree crown sizes, and most of coconut trees in the training dataset are belong to the general tree crown size. Therefore, our model learns less representations and features of small coconut trees and large coconut trees. Additionally, coconut trees with larger crown sizes or smaller crown sizes are more easier to be overlapped by other coconut trees, which causes unavoidable performance deterioration.
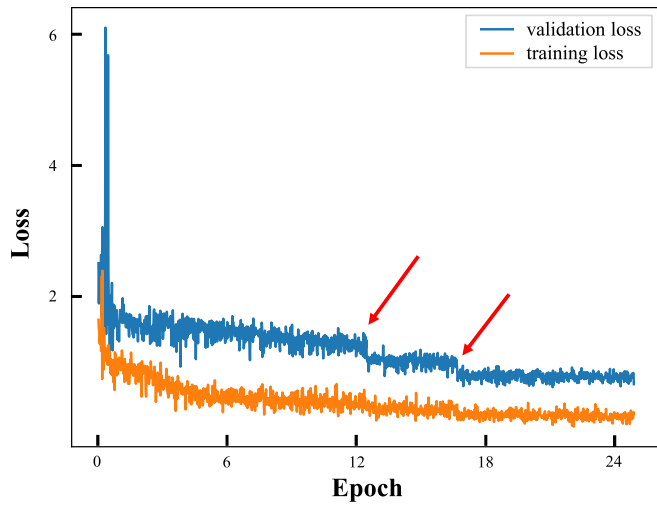
Fig. 14. The training loss and validation loss for training process of our proposed COCODET.

5.1.3. Relationship between coconut tree detection performance and the elevation value

In this section, we analyze the detection performance under different DEM. As shown in Fig. 17, we display the relationship between the detection performance and the elevation of these coconut palms using NASA STRM (Rodriguez et al., 2006). We can observe that the detection performance is better with a higher DEM. The reason maybe that the layout of coconut trees in the higher DEM is kind of sparse than that in the lower DEM, with less sheltering or overlapping with each other. In addition, a higher DEM is generally located far from the sea line, which may reduce the number of confusions with other land cover types or with shadows of coconut trees.

5.2. Connections between coconut tree distribution and the ecology

Table 9 summarizes the number of coconut palms and the density (trees per ha) for these four atolls in the Acteon Group. We can observe that the Tenararo contains the most coconut trees with 41,171 detected by our algorithm across the whole atoll. In addition, the coconut density of the Tenararo achieves 151 trees per ha, which is far higher than other

three atolls. Fig. 19 shows the density distribution for these four atolls. Tenararo has the largest number of birds and other threatened species, as well as introduced mammals ((Blanvillain, 2000; Blanvillain et al., 2002)). For example, Polynesia ground doves have a population size of about 120 globally, and most of them are living in Tenararo.

Fig. 18 shows the coconut canopy cover area and coconut canopy cover percent for these four atolls in the Acteon Group. These four atolls' coconut canopy cover area is 228 ha, 133 ha, 160 ha and 167 ha, respectively. According to our detection results, Tenararo has the highest canopy cover percentage of 84%. The percentage vegetation cover is higher than recorded previously (see (Blanvillain et al., 2002; Pierce and Blanvillain, 2004; Griffiths et al., 2008; Sayre et al., 2019)), especially for Tenararo (39% vs. 84%) and Matureivavao (14% vs. 42%). As for Vahanga and Tenarunga, the previous recorded vegetation percentages is only slightly lower than our results, with 30% vs. 35% and 32% vs. 38%, respectively. According to the satellite images shown in Fig. 5 and the 10 m land cover / land use product (Karra et al., 2021), our results are more accurate than those previously reported.

Based our coconut palm detection results, we provide a series of tree density distribution maps in Fig. 19, with spatial resolution of 500 m, 100 m and 10 m (from top to bottom). Because other vegetated areas (e. g. shrubland) have low cover (15% (Karra et al., 2021)), these coconut palm density maps are almost equal to real tree density maps. Compared to a global tree density map with a spatial resolution of 1 km from Crowther et al. (2015) (see Fig. 20), our density maps are more accurate and applicable for environmental and ecological analysis. Our tree detection results and density maps are available on https://github.com/rs-dl/coconut_in_Acteon_Group and we hope that our results will be helpful for those researchers who are interested in the Acteon Group.

From the tree density map in Fig. 19, it is observable that the tree density in the southwest direction is quite low for all these four atolls. As shown in Fig. 21, we describe the land area (a-d), canopy area (e-h) and canopy percentage (i-l) for four atolls. Initially, all these atolls are complete circles from volcanic vent, while they gradually open loopholes as time goes by. These loopholes mainly locate at the southwest corner and cause a low canopy cover. Explanations for low canopy cover in the southwest direction may be the result of damage by ocean currents or other damages.

If we do not do anything, the loopholes may become larger and larger, and the land area will accelerate to disappear. To this end, the situation for these four atolls will be more vulnerable and dangerous, and many special species will be under threat because of the missing
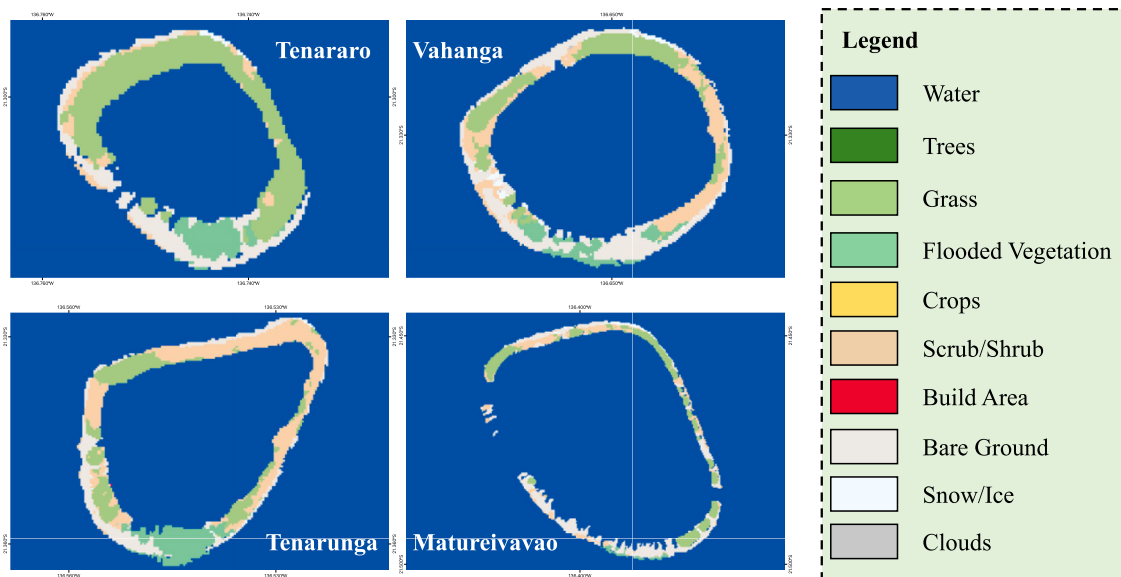

Fig. 15. The land cover mapping results of four remote atolls in the Acteon Group from ESRA 10 m product (Karra et al., 2021).
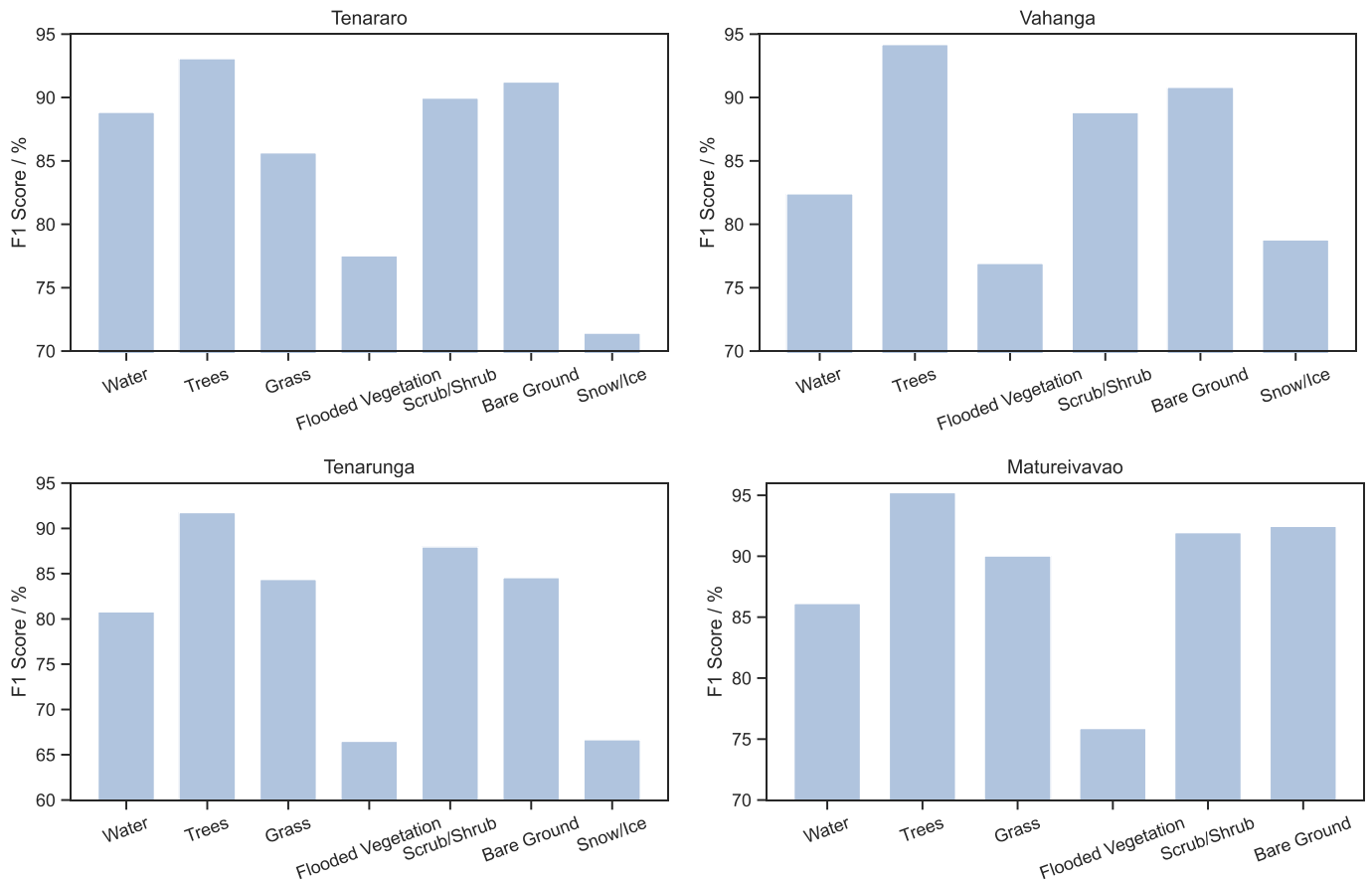
Fig. 16. The relationship between the F1 score and the land cover types for four atolls in the Acteon Group using our proposed COCODET. We use ESRI 10 m (Karra et al., 2021) as the land cover mapping.

Table 8
The precisions of coconut detection under different sizes of tree crowns using our proposed COCODET.

Crown size		Tenararo	Vahanga	Tenarunga	Matureivavao
Small tree crown size	TP	201	242	392	198
	FP	295	229	403	202
	Precision	40.52%	51.38%	49.31%	49.50%
	Average Precision	47.68%			
General tree crown size	TP	31,978	19,336	25,124	26,064
	FP	3519	2961	4983	2937
	Precision	90.09%	86.72%	83.45%	89.87%
	Average Precision	87.53%			
Large tree crown size	TP	134	175	273	166
	FP	70	84	197	74
	Precision	65.69%	67.57%	58.09%	67.17%
	Average Precision	65.13%			

habitat. For example, the breach in the southwest of the Matureivavao may accelerate to ruin the environment of the northeast of this island, where the land and the canopy area are both lower than other directions. In fact, the Matureivavao has the lowest number of native species, such as Polynesian dove and atoll fruit dove. The Tenararo and the Vahanga, which are considered as an Important Bird Area and a Key Biodiversity Area (Griffiths et al., 2011), have more complete land area and more canopy cover area.

5.3. The impacts of abandoned coconut plantations in the Acteon group

In this revision, we have added a section to discuss the impact of coconut plantations on the biodiversity in these four remote atolls. As introduced before, the Ackeon Group of atolls in French Polynesia of the Pacific Ocean (Fig. 5) is home to several threatened and near-threatened bird species, such as Polynesian grounddove (*Gallicolumba erythroptera*) and Tuamotu sandpiper (*Prosobonia cancellata*). The abandoned coconut plantation are important habitats for these endangered birds. Table 10 lists the endangered bird species (such as Polynesian ground dove, atoll fruit dove and Tuamotu sandpiper) observed on these four atolls in Griffiths et al. (2008). We can find that the Tenararo holds the best habitat for these threatened and near-threatened bird species, with significantly higher numbers than on the other three atolls, including Vahanga, Tenarunga and Matureivavao. In the meantime, we notice that the Tenararo has the highest density and canopy area of coconut plantations (see Fig. 18 and Table 9), proving that the importance of coconut plantations for these endangered bird species. To this end, the benefits of coconut plantations are threefold:

(1) The abandoned coconut plantations provide a vital habitat for many endangered bird species, but also provide safe havens to prevent Pacific rats and cats from eating their eggs of these threatened and near-threatened birds species.

(2) The abandoned coconut plantations provide good growth environment of Pisonia and Achyranthes, which many endangered bird species prefer for food, in between the rows of coconut palms, with enough nutrients and free from storm destruction.

(3) The abandoned coconut plantations also help to reduce the land and vegetation loss from dramatic effect of swells or other climate change phenomenon, which have been proved the negative effects of sea
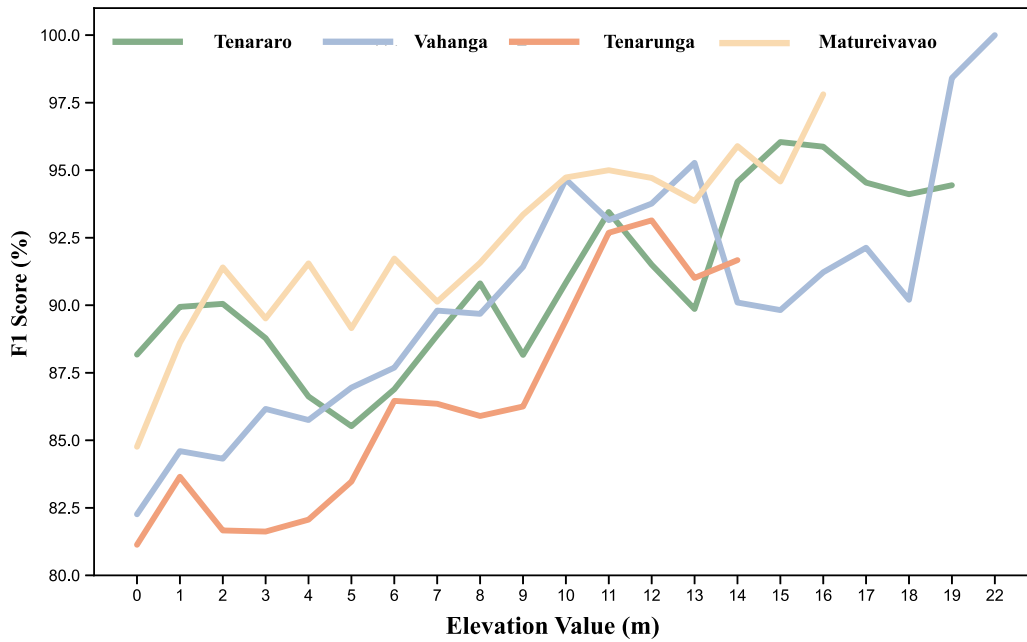
Fig. 17. The relationship between the F1 score and the elevation value for four atolls in the Acteon Group using our proposed COCODET. We use NASA STRM (Rodriguez et al., 2006) as our DEM product.

Table 9
The tree number and the density (trees per ha) for four atolls in the Acteon Group. The density is calculated as tree number / total land area.

Index	Tenararo	Vahanga	Tenarunga	Matureivavao	Overall
Tree Number	41,171	24,085	28,838	30,162	124,256
Density (tree per ha)	151.36	63.05	67.85	76.17	84.24

leval rises to the species (Lees et al., 2022).

However, coconut plantations in these four remote atolls of the Pacific Ocean also have some negative impacts for endangered bird species. The establishment of coconut plantations can increase the frequency of human visits to islands and consequently the likelihood of predator introduction. In addition, visiting birdwatchers, as well as local fishermen and coconut crab Birgus latro harvesters, may accidentally introduce rats, invasive ants, etc. which pose a threat to many endangered bird species as they colonise these atolls.

5.4. The transferability of COCODET for coconut tree crown detection

This section details and examines the transferability of COCODET. We have 12 transfer tasks in the experiment. For example, we train the COCODET using training data from each atoll in the Acteon Group (for example, the Tenararo (TA)) and test it on three distant atolls (for example, the Vahanga (VA), Tenarunga (TU), and Matureivavao (MA)). In this case, we have three transfer tasks: TA → VA, TA → TU, and TA → MU. It is noteworthy that the last column of 'All" in Fig. 22 means the average F1 score of four transfer tasks, and the last row of 'All" means the training set contains all four atolls, which is the same as reported in Table 3. Fig. 22 illustrates the transfer matrix of F1 score for all our transfer tasks. The atoll names in the left of the matrix represent the source domain (training region) while the atoll names below the matrix represent the target domain (test region). The model trained from one atoll cause $-7.5 \sim -12.43\%$ deterioration compared to the model trained from all atolls with respect to the F1 score. The best performance comes from local training, but training with all datasets achieves a satisfactory performance, that is only lower than the F1 scores along the diagonal of the matrix. Obviously, there exists serious domain gaps among these four remote atolls according to the accuracy of transfer tasks, although their sensors and spatial resolution are identical.
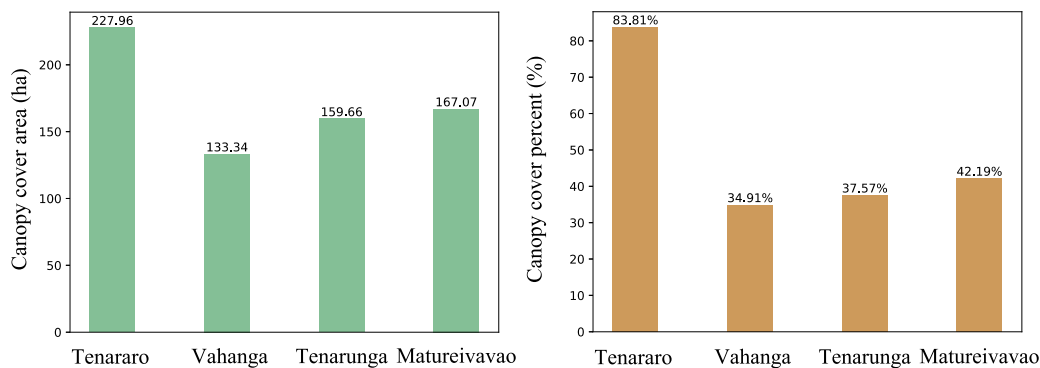

Fig. 18. The coconut canopy cover area and the coconut canopy cover percent for these four atolls in the Acteon Group. The canopy cover percent is calculated as canopy cover area / total land area.
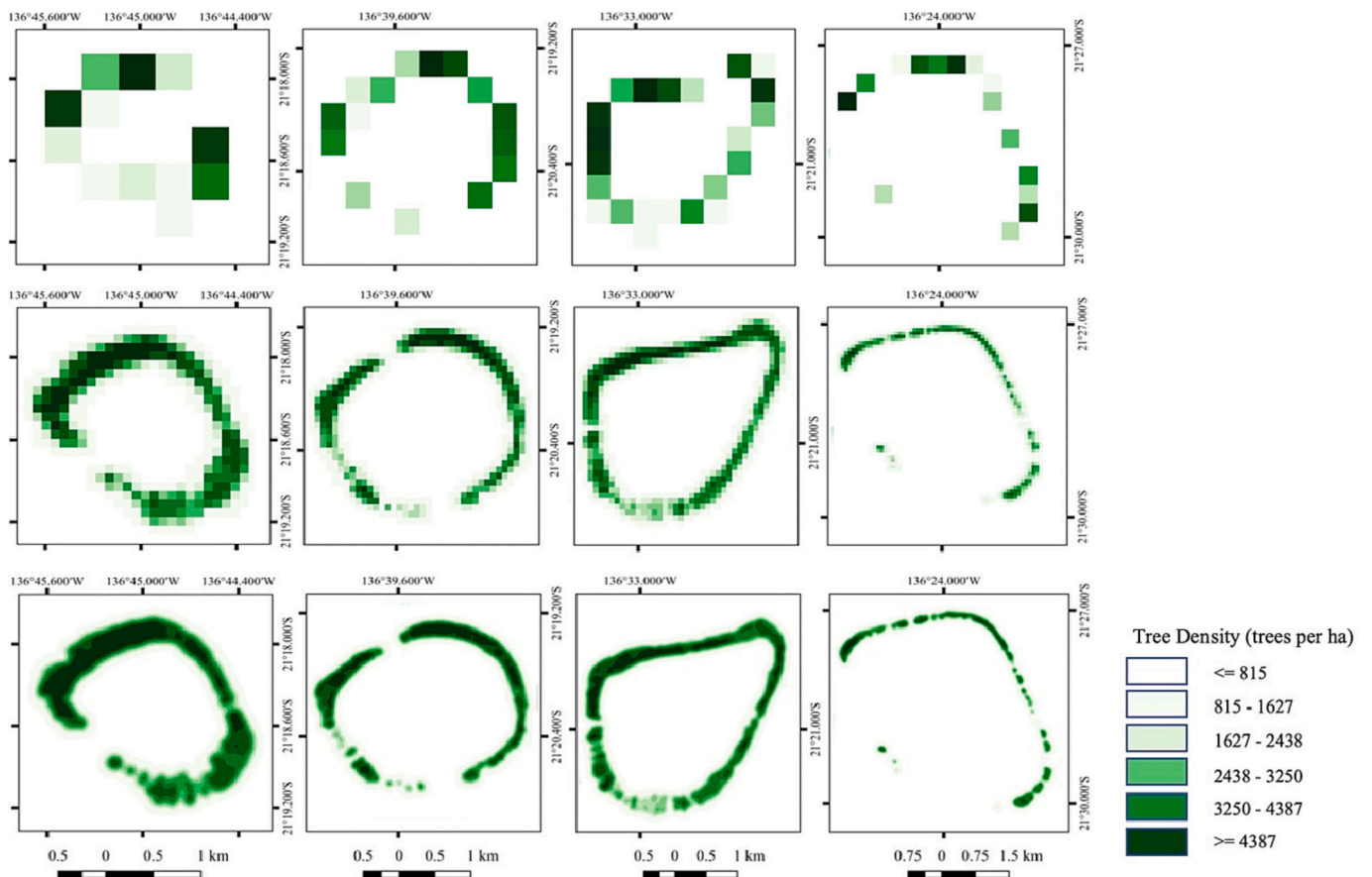
Fig. 19. The density distribution for these four atolls in the Acteon Group. The spatial resolutions of the top row, the middle row and the bottom row are 500 m, 100 m and 10 m. From left to right, the atolls are Tenararo, Vahanga, Tenarunga and Matureivavao, respectively.
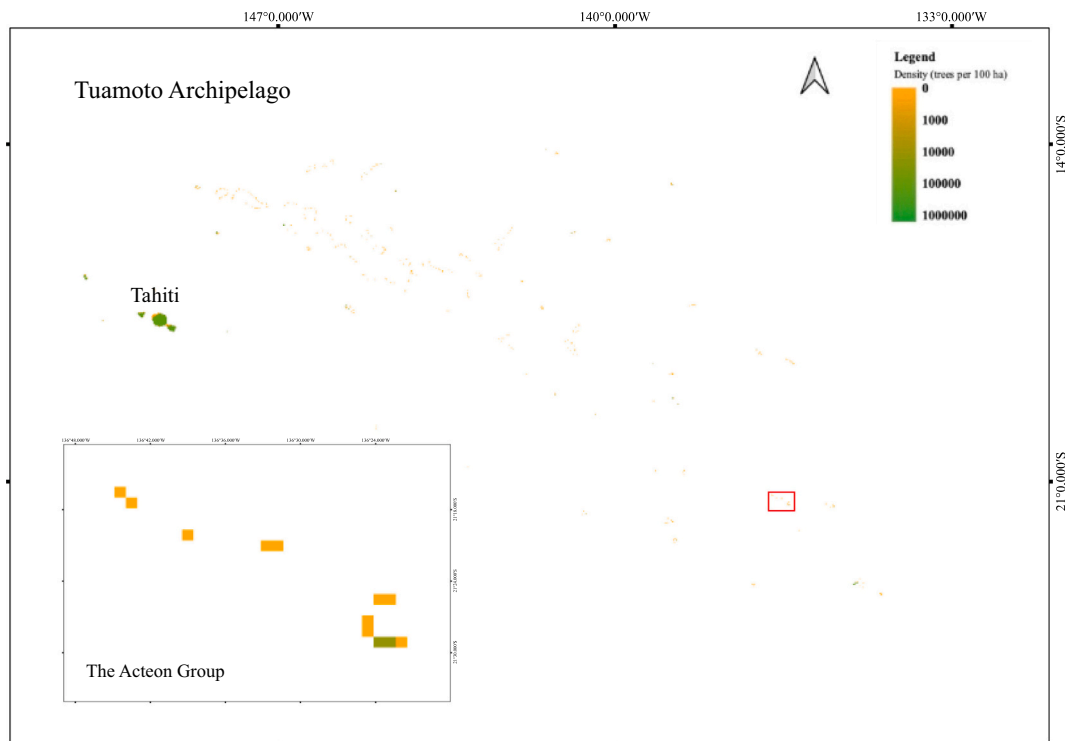

Fig. 20. The density distribution of coconuts with a spatial resolution of 1 km for four atolls in the Acteon Group, taken from Crowther et al. (2015).
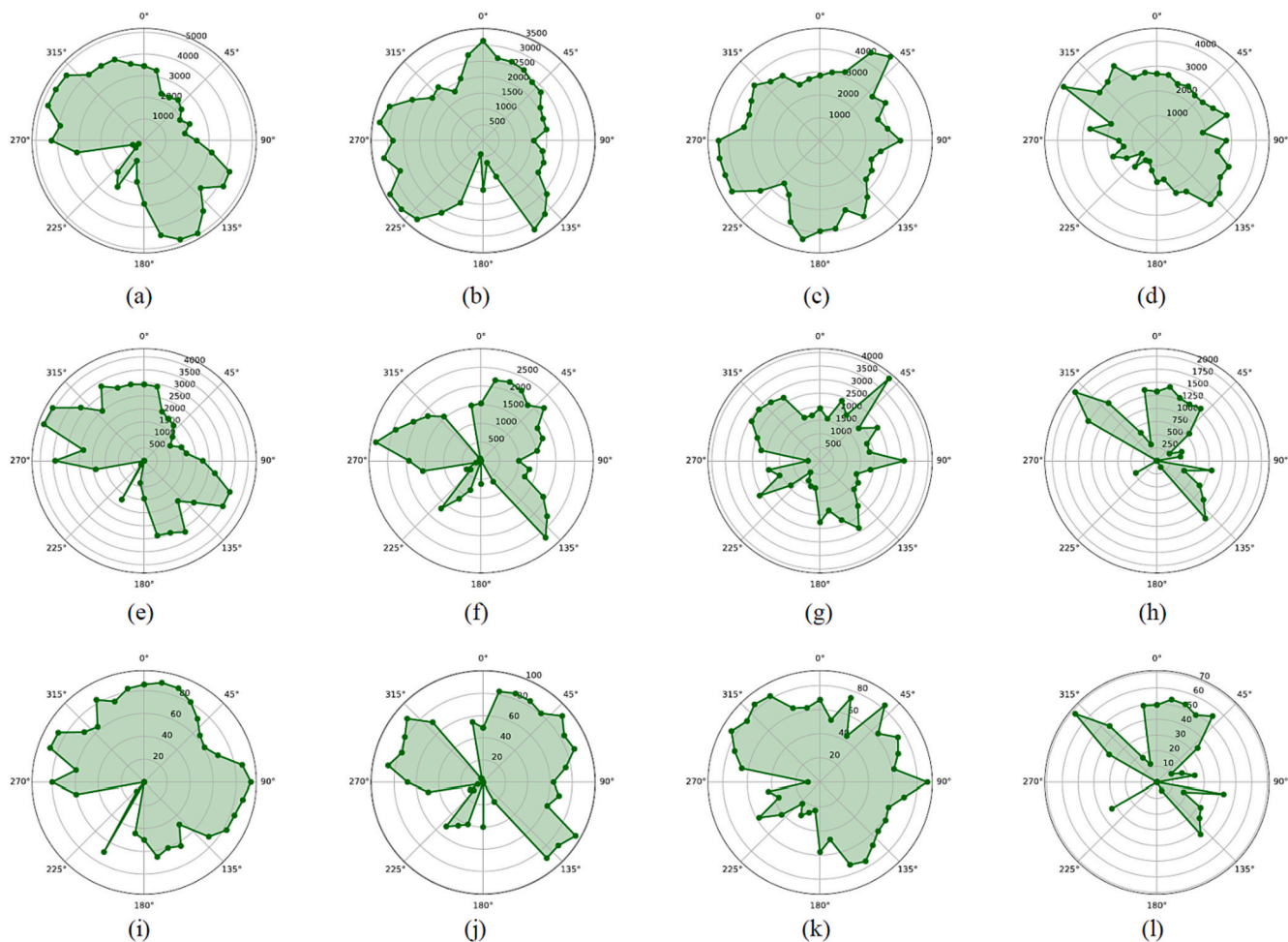
Fig. 21. A radar map of the land, canopy and the canopy percentage for these four atolls. (a)-(d): The radar map of the land area for the Tenararo, Vahanga, Tenarunga and Matureivavao, respectively. (e)-(h): The radar map of the canopy area for these four atolls. (i)-(l): The radar map of the canopy percentage (Unit: %) for these four atolls.

Table 10
The endangered bird species observed on Tenararo, Vahanga, Tenarunga and Matureivavao in Griffiths et al. (2008).

Bird species	Tenararo	Vahanga	Tenarunga	Matureivavao
Polynesia ground dove	20 ~ 50	1 ~ 2	0	0
Atoll fruit dove	100+	1 ~ 2	0	No record
Tuamotu sandpiper	600 ~ 1000	2 ~ 3	1	Few

Owing to the domain shift problem (Tong et al., 2020; Zheng et al., 2021c, 2022c), where each domain's own context information with specialty, spectral characteristics, and changeable environment, it's difficult to use vanilla training models without transferable tricks to another domain, contributing to a significant drop in detection accuracy. Recently, the issue of domain adaptation and domain generalization have been extensively discussed and explored in remote sensing community. However, the same issue in the cross-temporal or crossregional ITCD area has received little attention (Zheng et al., 2020; Wu et al., 2020a; Zheng et al., 2022a). More sophisticated, resilient, and generic algorithms for cross-temporal, cross-regional, or crossinstrument ITCD need to be developed and explored in the future.
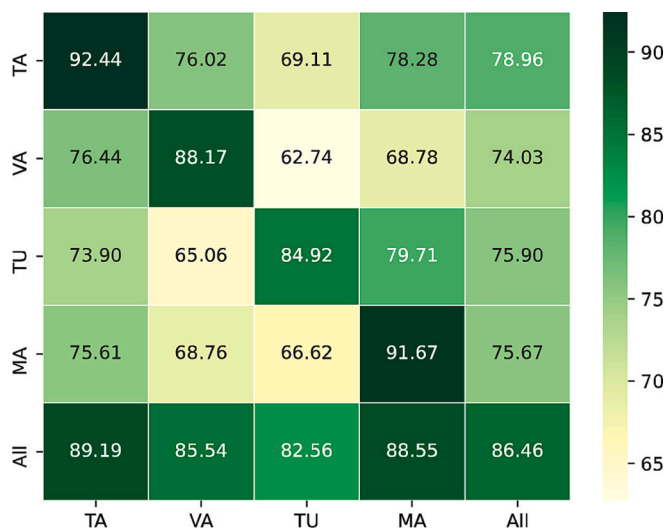

Fig. 22. The transfer matrix of F1 score for coconut tree crown detection in four remote atolls in the Acteon Group. The atoll names in the left of the matrix represent the source domain (training region) while the atoll names below the matrix represent the target domain (test region). TA, VA, TU, MA denotes Tenararo, Vahanga, Tenarunga and Matureivavao, respectively. "All" denotes the training set contains all four atolls, which is the same as reported in Table 3.

5.5. Potential future works

COCODET is an effective individual tree crown detection algorithm which is capable of highly accurate coconut tree crown detection (see Sec. 4.2.2). Future work could extend beyond the utilization of RGB-band satellite images that only represent the context semantic information and features, such as blue water, green vegetation or trees, and coconut-shape characteristics. Multi-spectral remote sensing images have a stronger capacity for capturing inherent features of coconut crowns and recognizing their growing status (Holmgren et al., 2008; Dash et al., 2017; Johansen et al., 2020). Our algorithm makes contributions to distinguishing coconut trees from other vegetation and detecting coarsely pixelated tree crowns through enhancing the feature representation with multi-scale feature fusion. COCODET is currently limited to detecting coconut trees in another different areas or images (Sec. 5.4) and a future step is to employ adversarial learning and transferable attention mechanism to enhance the model's transferability and generalization. This would broaden COCODET's applications, allowing it to be employed to detect other tree species, such as oil palm tree (Mubin et al., 2019), urban trees (Erker et al., 2019), or be used in agricultural applications, such as yield prediction (Nevavuori et al., 2019) and crop mapping (Xu et al., 2021a; Lin et al., 2022). Furthermore, we may extend coconut tree detection to a global scale. We can use globally available remotely sensed data (such as Sentinel, Landsat, MODIS, NASA GEDI, etc.) to map global coconut plantation at first, and then guide us to determine the approximate scope for counting individual coconut trees from higher-resolution remote sensing images.

6. Conclusions

In this study, we present a relatively more accurate coconut tree detection method - COCODET – that comprises of three main parts. First, we design an Adaptive Feature Enhancement (AFE) module for improving the capacity of representation at the highest level of feature map. AFE improves the feature representation ability at the highest level of the feature map, which contributes to better distinguish between coconut trees and other tree species or vegetation. Second, we modify the original RPN as T-RPN for producing coconut tree candidates. Finally, we propose a Cross Scale Fusion (CSF) module for integrating multi-scale information to improve the performance of detecting small coconut tree crowns, which benefits to fuse different level features of coconut tree crowns and achieve the connections between shallow and deep level semantic features. We detected all coconut trees in four remote atolls in the Acteon Group of the Pacific Ocean using our proposed COCODET and high-resolution satellite imagery. Our approach achieves an impressive detection accuracy with an average F1 score of 86.46% during a real-time inference process. Our ablation experiments demonstrate that our AFE, T-RPN and CSF considerably increase the detection accuracy. Our proposed COCODET outperforms other SOTA object detection methods with an improvement of 4.33 ~ 12.02% via the index of the average F1 score.

In these four atoll islands, we detect 120,237 individual coconut palm trees (84 trees per hectare), with 688 ha of coconut canopy cover in total. There are many threatened and near-threatened species living on these islands, such as the Polynesian ground dove (*Gallicolumba erythroptera*) and Tuamotu sandpiper (*Prosobonia cancellata*). To this end, all our detected coconut trees are held as a database that lays the foundation for ecological and preservation fieldwork and a comprehensive understanding of the ecosystem and biodiversity of the remote atolls. According to coconut detection results and the statistics from bird scientists, we can find that Tenararo holds the best habitat for these threatened and near-threatened bird species, with much more amount than other three atolls, including Vahanga, Tenarunga and Matureivavao. In the meantime, we notice that the Tenararo has the highest density and canopy area of coconut plantations, which prove that the importance of coconut plantations for these endangered bird species.

Also, we explore both the positive and negative impacts of abandoned coconut plantations in these four atolls. Furthermore, based our coconut detection results, we also provide a series of tree density distribution maps and it is observable that there exist loopholes in the southwest direction for all these four atolls. It calls attention to take some actions to protect these remote atolls, preventing the loopholes from becoming larger and larger. Therefore, accurate monitoring of coconut trees in these remote atolls from remote sensing images is quite essential to know the development of the expanding of these loopholes and the growing status of coconut trees.

Remote sensing technique and artificial intelligence algorithms show great potential for accurately observing and conveniently analyzing the environmental and ecological impacts in real-time. Furthermore, we will use multi-temporal or multi-source remote sensing images in the future, to achieve time-series monitoring trees and their growth status, not only in the Acteon Group, but also in other remote atolls in the Pacific Ocean. Long time series and real time monitoring of trees in these remote atolls could really help us to precisely analyze the wildlife biodiversity, carbon stock, environmental protection, and natural disasters, etc.

CRediT authorship contribution statement

Juepeng Zheng: Conceptualization, Methodology, Validation, Formal analysis, Investigation, Data curation, Writing – original draft, Writing – review & editing, Visualization. **Shuai Yuan:** Validation, Formal analysis, Investigation, Data curation, Writing – original draft, Visualization. **Wenzhao Wu:** Validation, Formal analysis, Investigation, Data curation. **Weijia Li:** Validation, Formal analysis, Investigation, Writing – review & editing. **Le Yu:** Conceptualization, Methodology, Resources, Writing – review & editing, Supervision, Project administration, Funding acquisition. **Haohuan Fu:** Conceptualization, Methodology, Resources, Writing – review & editing, Supervision, Project administration, Funding acquisition. **David Coomes:** Methodology, Writing – review & editing.

Declaration of Competing Interest

The authors declare that they have no known competing financial interests or personal relationships that could have appeared to influence the work reported in this paper.

Data availability

Data will be made available on request.

Appendix A. Supplementary data

Supplementary data to this article can be found online at https://doi.org/10.1016/j.rse.2023.113485.

References

Abankwah, V., Aidoo, R., Tweneboah-Koduah, B., 2010. Margins and economic viability of fresh coconut marketing in the Kumasi metropolis of Ghana. J. Dev. Agric. Econ. 2, 432–440.

Ampatzidis, Y., Partel, V., Meyering, B., Albrecht, U., 2019. Citrus rootstock evaluation utilizing UAVbased remote sensing and artificial intelligence. Comput. Electron. Agric. 164, 104900.

Blanvillain, C., 2000. Post-doctorat sur l'etude et la sauvegarde des oseaux endemiques de polynesie francaise. Rapport final d'activite, 2001.

Blanvillain, C., Florent, C., Thenot, V., 2002. Land birds of tuamotu archipelago, polynesia: relative abundance and changes during the 20th century with particular reference to the critically endangered polynesian ground-dove (gallicolumba erythroptera). Biol. Conserv. 103, 139–149.

Brandt, M., Rasmussen, K., Hiernaux, P., Herrmann, S., Tucker, C.J., Tong, X., Tian, F., Mertz, O., Kergoat, L., Mbow, C., et al., 2018. Reduction of tree cover in West African woodlands and promotion in semi-arid farmlands. Nat. Geosci. 11, 328–333.

Brandt, M., Tucker, C.J., Kariryaa, A., Rasmussen, K., Abel, C., Small, J., Chave, J., Rasmussen, L.V., Hiernaux, P., Diouf, A.A., et al., 2020. An unexpectedly large count of trees in the West African Sahara and Sahel. Nature 587, 78–82.

Brooke, M.D.L., Hilton, G., Martins, T., 2007. Prioritizing the world's islands for vertebrate-eradication programmes. Anim. Conserv. 10, 380–390.

Cai, Z., Vasconcelos, N., 2019. Cascade r-cnn: high quality object detection and instance segmentation. IEEE Trans. Pattern Anal. Mach. Intell. 43, 1483–1498.

Chen, K., Wang, J., Pang, J., Cao, Y., Xiong, Y., Li, X., Sun, S., Feng, W., Liu, Z., Xu, J., 2019. Mmdetection: Open mmlab detection toolbox and benchmark. arXiv preprint arXiv:1906.07155.

Chong, K.L., Kanniah, K.D., Pohl, C., Tan, K.P., 2017. A review of remote sensing applications for oil palm studies. Geo-spat. Inform. Sci. 20, 184–200.

Crowther, T.W., Glick, H.B., Covey, K.R., Bettigole, C., Maynard, D.S., Thomas, S.M., Smith, J.R., Hintler, G., Duguid, M.C., Amatulli, G., et al., 2015. Mapping tree density at a global scale. Nature 525, 201–205.

Curlew, B.-T., 2014. Bristle-thighed curlew and tuamotu sandpiper: two endangered shore-birds from the south pacific. Dutch Birding 36, 178–187.

Dahl, A.L., 1986. Review of the Protected Areas System in Oceania. IUCN, Gland, Switzerland.

Dalponte, M., Ørka, H.O., Ene, L.T., Gobakken, T., Næsset, E., 2014. Tree crown delineation and tree species classification in boreal forests using hyperspectral and als data. Remote Sens. Environ. 140, 306–317.

Danso, H., 2017. Properties of coconut, oil palm and bagasse fibres: as potential building materials. Proc. Eng. 200, 1–9.

Dash, J.P., Watt, M.S., Pearse, G.D., Heaphy, M., Dungey, H.S., 2017. Assessing very high resolution uav imagery for monitoring forest health during a simulated disease outbreak. ISPRS J. Photogramm. Remote Sens. 131, 1–14.

DATA, I.B., 2006. Cepf small grant final project completion report. development.

Dong, T., Shen, Y., Zhang, J., Ye, Y., Fan, J., 2019. Progressive cascaded convolutional neural networks for single tree detection with Google Earth imagery. Remote Sens. 11, 1786.

Erker, T., Wang, L., Lorentz, L., Stoltman, A., Townsend, P.A., 2019. A statewide urban tree canopy mapping method. Remote Sens. Environ. 229, 148–158.

Gebreslasie, M., Ahmed, F., Van Aardt, J.A., Blakeway, F., 2011. Individual tree detection based on variable and fixed window size local maxima filtering applied to ikonos imagery for even-aged eucalyptus plantation forests. Int. J. Remote Sens. 32, 4141–4154.

Gibril, M.B.A., Shafri, H.Z.M., Shanableh, A., Al-Ruzouq, R., Wayayok, A., Hashim, S.J., 2021. Deep convolutional neural network for large-scale date palm tree mapping from UAV-based images. Remote Sens. 13, 2787.

Gleason, C.J., Im, J., 2012. Forest biomass estimation from airborne lidar data using machine learning approaches. Remote Sens. Environ. 125, 80–91.

Gougeon, F.A., Leckie, D.G., 2006. The individual tree crown approach applied to ikonos images of a coniferous plantation area. Photogramm. Eng. Remote Sens. 72, 1287–1297.

Griffiths, R., Gideon, C., Gouni, A., 2008. Ecological restoration of vahanga atoll, acteon group, tuamotu archipelago. Department of Conservation, Wellington, New-Zealand, Société d'Ornithologie de Polynésie, Taravao, French Polynesia.

Griffiths, R., Miller, A., Climo, G., 2011. Addressing the impact of land crabs on rodenteradications on islands. Pac. Conserv. Biol. 17, 347–353.

Guirado, E., Tabik, S., Alcaraz-Segura, D., Cabello, J., Herrera, F., 2017. Deep-learning versus obia for scattered shrub detection with google earth imagery: Ziziphus lotus as case study. Remote Sens. 9, 1220.

Guo, C., Fan, B., Zhang, Q., Xiang, S., Pan, C., 2020. AugFPN: improving multi-scale feature learning for object detection.. In: Proceedings of the IEEE/CVF Conference on Computer Vision and Pattern Recognition, pp. 12595–12604.

Gurumurthy, V.A., Kestur, R., Narasipura, O., 2019. Mango tree net–a fully convolutional network for semantic segmentation and individual crown detection of mango trees. arXiv preprint arXiv:1907.06915.

Hansen, M.C., Potapov, P.V., Moore, R., Hancher, M., Turubanova, S.A., Tyukavina, A., Thau, D., Stehman, S., Goetz, S.J., Loveland, T.R., et al., 2013. High-resolution global maps of 21st-century forest cover change. Science 342, 850–853.

Hao, Z., Lin, L., Post, C.J., Mikhailova, E.A., Li, M., Chen, Y., Yu, K., Liu, J., 2021. Automated tree-crown and height detection in a young forest plantation using mask region-based convolutional neural network (mask R-CNN). ISPRS J. Photogramm. Remote Sens. 178, 112–123.

He, K., Zhang, X., Ren, S., Sun, J., 2016. Deep residual learning for image recognition. In: Proceedings of the IEEE Conference on Computer Vision and Pattern Recognition, pp. 770–778.

Heenkenda, M.K., Joyce, K.E., Maier, S.W., 2015. Mangrove tree crown delineation from high-resolution imagery. Photogramm. Eng. Remote Sens. 81, 471–479.

Holmgren, J., Persson, A., Soderman, U., 2008. Species identification of individual trees by combining high resolution lidar data with multi-spectral images. Int. J. Remote Sens. 29, 1537–1552.

Hu, J., Shen, L., Sun, G., 2018. Squeeze-and-excitation networks. In: Proceedings of the IEEE Conference on Computer Vision and Pattern Recognition, pp. 7132–7141.

Hung, C., Bryson, M., Sukkarieh, S., 2012. Multi-class predictive template for tree crown detection. ISPRS J. Photogramm. Remote Sens. 68, 170–183.

Itakura, K., Hosoi, F., 2020. Automatic tree detection from three-dimensional images reconstructed from 360 spherical camera using yolo v2. Remote Sens. 12, 988.

Johansen, K., Duan, Q., Tu, Y.-H., Searle, C., Wu, D., Phinn, S., Robson, A., McCabe, M.F., 2020. Mapping the condition of macadamia tree crops using multi-spectral uav and worldview-3 imagery. ISPRS J. Photogramm. Remote Sens. 165, 28–40.

Kappally, S., Shirwaikar, A., Shirwaikar, A., 2015. Coconut oil–a review of potential applications. Hygeia JD Med 7, 34–41.

Karra, K., Kontgis, C., Statman-Weil, Z., Mazzariello, J.C., Mathis, M., Brumby, S.P., 2021. Global land use/land cover with sentinel 2 and deep learning. In: S. IEEE, pp. 4704–4707.

Koc-San, D., Selim, S., Aslan, N., San, B.T., 2018. Automatic citrus tree extraction from UAV images and digital surface models using circular hough transform. Comput. Electron. Agric. 150, 289–301.

Lathika, M., Ajith Kumar, C., 2005. Growth trends in area, production and productivity of coconut in India. Ind. J. Agric.Econ. 60.

Leckie, D.G., Walsworth, N., Gougeon, F.A., 2016. Identifying tree crown delineation shapes and need for remediation on high resolution imagery using an evidence based approach. ISPRS J. Photogramm. Remote Sens. 114, 206–227.

LeCun, Y., Bengio, Y., Hinton, G., 2015. Deep learning. Nature 521, 436–444.

Lees, A.C., Haskell, L., Allinson, T., Bezeng, S.B., Burfield, I.J., Renjifo, L.M., Rosenberg, K.V., Viswanathan, A., Butchart, S.H., 2022. State of the world's birds. Ann. Rev. Environ. Resourc. 47.

Li, W., Fu, H., Yu, L., Cracknell, A., 2017. Deep learning based oil palm tree detection and counting for high-resolution remote sensing images. Remote Sens. 9, 22.

Li, W., He, C., Fang, J., Zheng, J., Fu, H., Yu, L., 2019. Semantic segmentation-based building footprint extraction using very high-resolution satellite images and multi-source GIS data. Remote Sens. 11, 403.

Lin, C., Zhong, L., Song, X.-P., Dong, J., Lobell, D.B., Jin, Z., 2022. Early-and in-season crop type mapping without current-year ground truth: generating labels from historical information via a topologybased approach. Remote Sens. Environ. 274, 112994.

Lin, M., Chen, Q., Yan, S., 2013. Network in network. arXiv preprint arXiv:1312.4400.

Lin, T.-Y., Dollar, P., Girshick, R., He, K., Hariharan, B., Belongie, S., 2017. Feature pyramid networks for object detection. In: Proceedings of the IEEE Conference on Computer Vision and Pattern Recognition, pp. 2117–2125.

Lin, T.-Y., Goyal, P., Girshick, R., He, K., Dollar, P., 2018. Focal loss for dense object detection. IEEE Trans. Pattern Anal. Mach.Intell. 42, 318–327.

Liu, S., Qi, L., Qin, H., Shi, J., Jia, J., 2018. Path aggregation network for instance segmentation. In: Proceedings of the IEEE Conference on Computer Vision and Pattern Recognition, pp. 8759–8768.

Liu, Y., Zhao, J., Qin, Y., 2021. A novel technique for ship wake detection from optical images. Remote Sens. Environ. 258, 112375.

Lu, X., Li, B., Yue, Y., Li, Q., Yan, J., 2019. Grid R-CNN. In: Proceedings of the IEEE/CVF Conference on Computer Vision and Pattern Recognition, pp. 7363–7372.

Lumnitz, S., Devisscher, T., Mayaud, J.R., Radic, V., Coops, N.C., Griess, V.C., 2021. Mapping trees along urban street networks with deep learning and street-level imagery. ISPRS J. Photogramm. Remote Sens. 175, 144–157.

Malek, S., Bazi, Y., Alajlan, N., AlHichri, H., Melgani, F., 2014. Efficient framework for palm tree detection in uav images. IEEE J. Select. Top. Appl. Earth Observ. Remote Sens. 7, 4692–4703.

Meijaard, E., Abrams, J.F., Juffe-Bignoli, D., Voigt, M., Sheil, D., 2020. Coconut oil, conservation and the conscientious consumer. Curr. Biol. 30, R757–R758.

Miraki, M., Sohrabi, H., Fatehi, P., Kneubuehler, M., 2021. Individual tree crown delineation from high-resolution uav images in broadleaf forest. Ecol. Inform. 61, 101207.

Mohan, M., de Mendonca, B.A.F., Silva, C.A., Klauberg, C., de Saboya Ribeiro, A.S., de Araujo, E.J.G., Monte, M.A., Cardil, A., 2019. Optimizing individual tree detection accuracy and measuring forest uniformity in coconut (cocos nucifera l.) plantations using airborne laser scanning. Ecol. Model. 409, 108736.

Moulin, A., 1866. Notices sur les colonies fran̨caises. Mubin, N. A., Nadarajoo, E., Shafri, H. Z. M., & Hamedianfar, A. (2019). Young and mature oil palm tree detection and counting using convolutional neural network deep learning method. Int. J. Remote Sens. 40, 7500–7515.

Mubin, N.A., Nadarajoo, E., Shafri, H.Z.M., Hamedianfar, A., 2019. Young and mature oilpalm tree detection and counting using convolutional neural network deep learningmethod. Int. J. Remote Sens. 40 (19), 7500–7515.

Nevalainen, O., Honkavaara, E., Tuominen, S., Viljanen, N., Hakala, T., Yu, X., Hyyppa, J., Saari, H., Polonen, I., Imai, N.N., et al., 2017. Individual tree detection and classification with UAV-based photogrammetric point clouds and hyperspectral imaging. Remote Sens. 9, 185.

Nevavuori, P., Narra, N., Lipping, T., 2019. Crop yield prediction with deep convolutional neural networks. Comput. Electron. Agric. 163, 104859.

Ng, A., 2017. Improving deep neural networks: Hyperparameter tuning, regularization and optimization. Deeplearning. ai on Coursera.

Nguyen, H.T., Lopez Caceres, M.L., Moritake, K., Kentsch, S., Shu, H., Diez, Y., 2021. Individual sick fir tree (Abies Mariesii) identification in insect infested forests by means of UAV images and deep learning. Remote Sens. 13, 260.

Norzaki, N., Tahar, K.N., 2019. A comparative study of template matching, iso cluster segmentation, and tree canopy segmentation for homogeneous tree counting. Int. J. Remote Sens. 40, 7477–7499.

Nowell, C.E., 1968. The pacific basin: A history of its geographical exploration.

Oksuz, K., Cam, B.C., Kalkan, S., Akbas, E., 2020. Imbalance problems in object detection: a review. IEEE Trans. Pattern Anal. Mach. Intell. 43, 3388–3415.

Onishi, M., Ise, T., 2021. Explainable identification and mapping of trees using UAV RGB image and deep learning. Sci. Rep. 11, 1–15.

Osco, L.P., de Arruda, M.D.S., Junior, J.M., da Silva, N.B., Ramos, A.P.M., Moryia, E.A.S., Imai, N.N., Pereira, D.R., Creste, J.E., Matsubara, E.T., et al., 2020. A convolutional neural network approach for counting and geolocating citrus-trees in uav multispectral imagery. ISPRS J. Photogramm. Remote Sens. 160, 97–106.

Osco, L.P., Nogueira, K., Ramos, A.P.M., Pinheiro, M.M.F., Furuya, D.E.G., Goncalves, W. N., de Castro Jorge, L.A., Junior, J.M., dos Santos, J.A., 2021. In: Semantic segmentation of citrus-orchard using deep neural networks and multispectral uav-based imagery. Precision Agriculture, pp. 1–18.

Ouma, Y.O., Tateishi, R., 2008. Urban-trees extraction from quickbird imagery using multiscale spectex-filtering and non-parametric classification. ISPRS J. Photogramm. Remote Sens. 63, 333–351.

Panagiotidis, D., Abdollahnejad, A., Surovy, P., Chiteculo, V., 2017. Determining tree height and crown diameter from high-resolution UAV imagery. Int.J. Remote Sens. 38, 2392–2410.

Pang, J., Chen, K., Shi, J., Feng, H., Ouyang, W., Lin, D., 2019. Libra r-cnn: Towards balanced learning for object detection. In: Proceedings of the IEEE/CVF Conference on Computer Vision and Pattern Recognition, pp. 821–830.

Payne, M., 2021. Satellite remote sensing of deforestation for oil palm. Nat. Rev. Earth Environ. 2, 230.

Pearse, G.D., Tan, A.Y., Watt, M.S., Franz, M.O., Dash, J.P., 2020. Detecting and mapping tree seedlings in UAV imagery using convolutional neural networks and field-verified data. ISPRS J. Photogramm. Remote Sens. 168, 156–169.

Pierce, R., Blainvillain, C., Burle, M.-H., 2015. Bird research and monitoring associated with SOP Manu pest eradications in Acteon–Gambier archipelagos, June 2015. Unpublished Report. Suva, Fiji: BirdLife International, Pacific Secretariat.

Pierce, R., Blanvillain, C., 2004. Current status of the endangered tuamotu sandpiper or titi prosobonia cancellata and recommended actions for its recovery. Wader Study Group Bull. 105, 93–100.

Pitkänen, J., 2001. Individual tree detection in digital aerial images by combining locally adaptive binarization and local maxima methods. Can. J. For. Res. 31, 832–844.

Pott, M., Griffiths, R., Burle, M.-H., Wegmann, A., 2014. Protecting the tuamotu sandpiper (prosobonia cancellata) one island at a time. In: Proceedings of the Vertebrate Pest Conference, vol. 26. International Society for Optics and Photonics volume 11394.

Pu, R., Landry, S., 2012. A comparative analysis of high spatial resolution ikonos and worldview-2 imagery for mapping urban tree species. Remote Sens. Environ. 124, 516–533.

Puttemans, S., Van Beeck, K., Goedeme, T., 2018. Comparing boosted cascades to deep learning architectures for fast and robust coconut tree detection in aerial images. In: Proceedings of the 13th International 875 Joint Conference on Computer Vision, Imaging and Computer Graphics Theory and Applications, pp. 230–241. SCITEPRESS vol. 5.

Quanchi, M., Robson, J., 2005. Historical Dictionary of the Discovery and Exploration of the Pacific Islands. Scarecrow Press.

Rahnemoonfar, M., Sheppard, C., 2017. Deep count: fruit counting based on deep simulated learning. Sensors 17, 905.

Ren, S., He, K., Girshick, R., Sun, J., 2016. Faster R-CNN: towards real-time object detection with region proposal networks. IEEE Trans. Pattern Anal. Mach. Intell. 39, 1137–1149.

Rodriguez, E., Morris, C.S., Belz, J.E., 2006. A global assessment of the SRTM performance. Photogramm. Eng. Remote Sens. 72, 249–260.

Safonova, A., Tabik, S., Alcaraz-Segura, D., Rubtsov, A., Maglinets, Y., Herrera, F., 2019. Detection of fir trees (Abies Sibirica) damaged by the bark beetle in unmanned aerial vehicle images with deep learning. Remote Sens. 11, 643.

Santoso, H., Tani, H., Wang, X., 2016. A simple method for detection and counting of oil palm trees using high-resolution multispectral satellite imagery. Int. J. Remote Sens. 37, 5122–5134.

Sayre, R., Noble, S., Hamann, S., Smith, R., Wright, D., Breyer, S., Butler, K., Van Graafeiland, K., Frye, C., Karagulle, D., et al., 2019. A new 30 meter resolution global shoreline vector and associated global islands database for the development of standardized ecological coastal units. J. Operat. Oceanogr. 12, S47–S56.

Selvaraj, M.G., Vergara, A., Montenegro, F., Ruiz, H.A., Safari, N., Raymaekers, D., Ocimati, W., Ntamwira, J., Tits, L., Omondi, A.B., et al., 2020. Detection of banana plants and their major diseases through aerial images and machine learning methods: a case study in DR Congo and Republic of Benin. ISPRS J. Photogramm. Remote Sens. 169, 110–124.

Skurikhin, A.N., Garrity, S.R., McDowell, N.G., Cai, D.M., 2013. Automated tree crown detection and size estimation using multi-scale analysis of high-resolution satellite imagery. Remote Sens. Lett. 4, 465–474.

de Souza, I.E., Falcão, A.X., 2022. Learning CNN filters from user-drawn image markers for coconut-tree image classification. IEEE Geosci. Remote Sens. Lett. 19, 1-5.

Sun, P., Zhang, R., Jiang, Y., Kong, T., Xu, C., Zhan, W., Tomizuka, M., Li, L., Yuan, Z., Wang, C., 2021. Sparse R-CNN: End-to-end object detection with learnable proposals. In: Proceedings of the IEEE/CVF Conference on Computer Vision and Pattern Recognition, pp. 14454–14463.

Teina, R., Bereziat, D., Stoll, B., Chabrier, S., 2008. Toward a global tuamotu archipelago coconut trees sensing using high resolution optical data. In: IGARSS 2008-2008 IEEE International Geoscience and Remote Sensing Symposium (pp. II–797). IEEE vol. 2.

Tochon, G., Feret, J.-B., Valero, S., Martin, R.E., Knapp, D.E., Salembier, P., Chanussot, J., Asner, G.P., 2015. On the use of binary partition trees for the tree crown segmentation of tropical rainforest hyperspectral images. Remote Sens. Environ. 159, 318–331.

Tong, X.-Y., Xia, G.-S., Lu, Q., Shen, H., Li, S., You, S., Zhang, L., 2020. Land-cover classification with high-resolution remote sensing images using transferable deep models. Remote Sens. Environ. 237, 111322.

Upendra, K., Panawala, P., Wickramasinghe, D., 2019. Automated coconut tree detection using UAV imageries. In: Proceedings of the 7th International Conference of Sabaragamuwa University of Sri Lanka (ICSUSL) (pp. 229–229). Sabaragamuwa University of Sri Lanka.

Vargas-Munoz, J.E., Zhou, P., Falcao, A.X., Tuia, D., 2019. Interactive coconut tree annotation using feature space projections.. In: IGARSS 2019-2019 IEEE International Geoscience and Remote Sensing Symposium. IEEE, pp. 5718–5721.

Veitch, C., Clout, M., Martin, A., Russell, J., West, C., 2019. Island Invasives: Scaling Up To Meet the Challenge. IUCN, Gland, Switzerland.

Vermote, E.F., Skakun, S., Becker-Reshef, I., Saito, K., 2020. Remote sensing of coconut trees in Tonga using very high spatial resolution worldview-3 data. Remote Sens. 12, 3113.

van der Vliet, R.E., Ghestemme, T., 2013. Endemic landbirds of French polynesia. Dutch Birding 35, 229–242.

Wallace, L., Sun, Q.C., Hally, B., Hillman, S., Both, A., Hurley, J., Saldias, D.S.M., 2021. Linking urban tree inventories to remote sensing data for individual tree mapping. Urban For. Urban Green. 61, 127106.

Wang, J., Chen, K., Yang, S., Loy, C.C., Lin, D., 2019. Region proposal by guided anchoring. In: Proceedings of the IEEE/CVF Conference on Computer Vision and Pattern Recognition, pp. 2965–2974.

Wang, Y., Zhu, X., Wu, B., 2019b. Automatic detection of individual oil palm trees from UAV images using hog features and an SVM classifier. Int. J. Remote Sens. 40, 7356–7370.

Weinstein, B.G., Marconi, S., Aubry-Kientz, M., Vincent, G., Senyondo, H., White, E.P., 2020a. Deep-forest: A python package for RGB deep learning tree crown delineation. Methods Ecol. Evol. 11, 1743–1751.

Weinstein, B.G., Marconi, S., Bohlman, S.A., Zare, A., White, E.P., 2020b. Cross-site learning in deep learning RGB tree crown detection. Ecol. Inform. 56, 101061.

Wu, W., Zheng, J., Fu, H., Li, W., Yu, L., 2020. Cross-regional oil palm tree detection. In: Proceedings of the IEEE/CVF Conference on Computer Vision and Pattern Recognition Workshops, pp. 56–57.

Wu, W., Zheng, J., Li, W., Fu, H., Yuan, S., Yu, L., 2020. Domain adversarial neural network-based oil palm detection using high-resolution satellite images. In: Automatic Target Recognition XXX, p. 1139406. International Society for Optics and Photonics volume 11394.

Xie, S., Girshick, R., Dollar, P., Tu, Z., He, K., 2017. Aggregated residual transformations for deep neural networks. In: Proceedings of the IEEE Conference on Computer Vision and Pattern Recognition, pp. 1492–1500.

Xu, J., Yang, J., Xiong, X., Li, H., Huang, J., Ting, K., Ying, Y., Lin, T., 2021a. Towards interpreting multi-temporal deep learning models in crop mapping. Remote Sens. Environ. 264, 112599.

Xu, X., Zhou, Z., Tang, Y., Qu, Y., 2021b. Individual tree crown detection from high spatial resolution imagery using a revised local maximum filtering. Remote Sens. Environ. 258, 112397.

Yang, Z., Liu, S., Hu, H., Wang, L., Lin, S., 2019. Reppoints: point set representation for object detection.. In: Proceedings of the IEEE/CVF International Conference on Computer Vision, pp. 9657–9666.

Young, J., 1899. Names of the paumotu islands, with the old names so far as they are known. J. Polynesian Soc. 8, 264–268.

Yuan, H., Huang, K., Ren, C., Xiong, Y., Duan, J., Yang, Z., 2022. Pomelo tree detection method based on attention mechanism and cross-layer feature fusion. Remote Sens. 14, 3902.

Zhang, C., Atkinson, P.M., George, C., Wen, Z., Diazgranados, M., Gerard, F., 2020. Identifying and mapping individual plants in a highly diverse high-elevation ecosystem using UAV imagery and deep learning. ISPRS J. Photogramm. Remote Sens. 169, 280–291.

Zhang, L., Dong, R., Yuan, S., Li, W., Zheng, J., Fu, H., 2021a. Making low-resolution satellite images reborn: a deep learning approach for super-resolution building extraction. Remote Sens. 13, 2872.

Zhang, T., Zhang, X., Liu, C., Shi, J., Wei, S., Ahmad, I., Zhan, X., Zhou, Y., Pan, D., Li, J., et al., 2021b. Balance learning for ship detection from synthetic aperture radar remote sensing imagery. ISPRS J. Photogramm. Remote Sens. 182, 190–207.

Zhao, H., Shi, J., Qi, X., Wang, X., Jia, J., 2017. Pyramid scene parsing network. In: Proceedings of the IEEE Conference on Computer Vision and Pattern Recognition, pp. 2881–2890.

Zhao, Z.-Q., Zheng, P., Xu, S.-T., Wu, X., 2019. Object detection with deep learning: a review. IEEE Trans. Neural Networks Learn. Syst. 30, 3212–3232.

Zheng, J., Fu, H., Li, W., Wu, W., Yu, L., Yuan, S., Tao, W.Y.W., Pang, T.K., Kanniah, K.D., 2021a. Growing status observation for oil palm trees using unmanned aerial vehicle (UAV) images. ISPRS J. Photogramm. Remote Sens. 173, 95–121.

Zheng, J., Fu, H., Li, W., Wu, W., Zhao, Y., Dong, R., Yu, L., 2020. Cross-regional oil palm tree counting and detection via a multi-level attention domain adaptation network. ISPRS J. Photogramm. Remote Sens. 167, 154–177.

Zheng, J., Li, W., Xia, M., Dong, R., Fu, H., Yuan, S., 2019. Large-scale oil palm tree detection from highresolution remote sensing images using FASTER-RCNN. In: IGARSS 2019–2019 IEEE International Geoscience and Remote Sensing Symposium. IEEE, pp. 1422–1425.

Zheng, J., Wu, W., Yu, L., Fu, H., 2021b. Coconut trees detection on the tenarunga using high-resolution satellite images and deep learning. In: In 2021 IEEE International Geoscience and Remote Sensing Symposium IGARSS. IEEE, pp. 6512–6515.

Zheng, J., Wu, W., Yuan, S., Fu, H., Li, W., Yu, L., 2022a. Multisource-domain generalization-based oil palm tree detection using very-high-resolution (vhr) satellite images. IEEE Geosci. Remote Sens. Lett. 19, 1–5.

Zheng, J., Wu, W., Zhao, Y., Yuan, S., Dong, R., Zhang, L., Fu, H., 2022b. A parallel approach for oil palm tree detection on a sw26010 many-core processor. In: IGARSS 2022–2022 IEEE International Geoscience and Remote Sensing Symposium. IEEE, pp. 1548–1551.

Zheng, J., Wu, W., Yuan, S., Zhao, Y., Li, W., Zhang, L., Dong, R., Fu, H., 2021c. A Two-Stage Adaptation Network (TSAN) for Remote Sensing Scene Classification in Single-Source-Mixed-Multiple-Target Domain Adaptation (S^{2}M^{2}T DA) Scenarios. IEEE Trans. on Geosci. and Remote Sens. 60, 1–13.

Zheng, J., Zhao, Y., Wu, W., Chen, M., Li, W., Fu, H., 2022c. Partial domain adaptation for scene classification from remote sensing imagery. IEEE Trans. Geosci. Remote Sens. 61, 1–17.